

University of Groningen

The time-reversal- and parity-violating nuclear potential in chiral effective theory

Maekawa, C. M.; Mereghetti, E.; de Vries, J.; van Kolck, U.

Published in:
 Nuclear Physics A

DOI:
[10.1016/j.nuclphysa.2011.09.020](https://doi.org/10.1016/j.nuclphysa.2011.09.020)

IMPORTANT NOTE: You are advised to consult the publisher's version (publisher's PDF) if you wish to cite from it. Please check the document version below.

Document Version
 Publisher's PDF, also known as Version of record

Publication date:
 2011

[Link to publication in University of Groningen/UMCG research database](#)

Citation for published version (APA):

Maekawa, C. M., Mereghetti, E., de Vries, J., & van Kolck, U. (2011). The time-reversal- and parity-violating nuclear potential in chiral effective theory. *Nuclear Physics A*, 872(1), 117-160.
<https://doi.org/10.1016/j.nuclphysa.2011.09.020>

Copyright

Other than for strictly personal use, it is not permitted to download or to forward/distribute the text or part of it without the consent of the author(s) and/or copyright holder(s), unless the work is under an open content license (like Creative Commons).

The publication may also be distributed here under the terms of Article 25fa of the Dutch Copyright Act, indicated by the "Taverne" license. More information can be found on the University of Groningen website: <https://www.rug.nl/library/open-access/self-archiving-pure/taverne-amendment>.

Take-down policy

If you believe that this document breaches copyright please contact us providing details, and we will remove access to the work immediately and investigate your claim.

Downloaded from the University of Groningen/UMCG research database (Pure): <http://www.rug.nl/research/portal>. For technical reasons the number of authors shown on this cover page is limited to 10 maximum.

The Time-Reversal- and Parity-Violating Nuclear Potential in Chiral Effective Theory

C.M. Maekawa¹, E. Mereghetti², J. de Vries³, and U. van Kolck²

¹ *Instituto de Matemática, Estatística e Física, Universidade Federal do Rio Grande
Campus Carreiros, PO Box 474, 96201-900 Rio Grande, RS, Brazil*

² *Department of Physics, University of Arizona, Tucson, AZ 85721, USA*

³ *KVI, Theory Group, University of Groningen, 9747 AA Groningen, The Netherlands*

Abstract

We derive the parity- and time-reversal-violating nuclear interactions stemming from the QCD $\bar{\theta}$ term and quark/gluon operators of effective dimension 6: quark electric dipole moments, quark and gluon chromo-electric dipole moments, and two four-quark operators. We work in the framework of two-flavor chiral perturbation theory, where a systematic expansion is possible. The different chiral-transformation properties of the sources of time-reversal violation lead to different hadronic interactions. For all sources considered the leading-order potential involves known one-pion exchange, but its specific form and the relative importance of short-range interactions depend on the source. For the $\bar{\theta}$ term, the leading potential is solely given by one-pion exchange, which does not contribute to the deuteron electric dipole moment. In subleading order, a new two-pion-exchange potential is obtained. Its short-range component is indistinguishable from one of two undetermined contact interactions that appear at the same order and represent effects of heavier mesons and other short-range QCD dynamics. One-pion-exchange corrections at this order are discussed as well.

1 Introduction

There are three sources of CP violation in the lowest-dimension operators of the Standard Model. Due to its flavor-changing properties, the phase of the CKM matrix is the best known and investigated source (see, for example, Ref. [1]). The recent discovery of neutrino masses opens up the possibility of analogous leptonic CP violation [2]. The third possible source comes from the $\bar{\theta}$ term in QCD [3]. Flavor-conserving quantities, in particular hadronic, nuclear, and atomic electric dipole moments (EDMs), are sensitive probes of this qualitatively different mechanism of CP violation. EDMs require the simultaneous violation of parity (P) and time-reversal (T); for a review, see Ref. [4].

Years of careful experimental investigation have set stringent bounds on the neutron EDM, $|d_n| < 2.9 \cdot 10^{-26} e \text{ cm}$ [5]. This upper limit points to a tiny value for the $\bar{\theta}$ parameter, $\bar{\theta} \lesssim 10^{-10}$, despite the naive-dimensional-analysis expectation that it be of $\mathcal{O}(1)$. Besides the neutron EDM, there are measurements on atomic EDMs. The leading contribution in a paramagnetic system comes from the EDM of the unpaired electron. In contrast, a diamagnetic atom has zero total electron angular momentum, and the main contribution to the atomic EDM comes from the nuclear Schiff moment (SM), the residual electron-nucleus interaction generated by the distribution of the EDM throughout the nuclear region. A less stringent bound on the proton EDM, $|d_p| < 7.9 \cdot 10^{-25} e \text{ cm}$, is extracted from the EDM of the ^{199}Hg atom [6] through a calculation of the nuclear SM [7]. Atomic EDMs can also receive contributions from higher nuclear moments that violate T , such as the magnetic quadrupole moment (MQM).

The unnaturally small value of $\bar{\theta}$ leaves room for other flavor-diagonal sources of T violation, which have their origin in physics beyond the Standard Model, at a high-energy scale M_T . Well below the new physics scale, these effects manifest themselves in interactions between Standard Model fields represented by higher-dimension T -violating (TV) operators, suppressed by more and more powers of M_T . We expect the most important TV effects to be captured by the operators of lowest dimension [8, 9, 10, 11], the dimension-6 quark electric and chromo-electric dipole moments (qEDM and qCEDM), gluon chromo-electric dipole moment (gCEDM), and TV four-quark (FQ) operators.

A recent renewal of the longstanding interest in EDMs comes from a new generation of experiments, which will improve the precision of EDM observables significantly. It is expected that the current bound on the neutron EDM will be pushed down to $10^{-27} - 10^{-28} e \text{ cm}$ [12] using high-density ultra-cold neutron sources at SNS [13] and ILL+PSI [14]. It has also been proposed that the EDM of charged particles could be measured in storage-ring experiments [15]. In addition to the proton, we could see a measurement of the deuteron EDM with a projected precision of $|d_d| \lesssim 10^{-29} e \text{ cm}$. A measurement on ^3He is also a possibility. These measurements probe dimension-6 sources at scales comparable to the scale reached at the LHC, so they could very well turn up positive signals.

Calculating hadronic and nuclear EDMs (and higher moments) directly from QCD with TV sources is a daunting task, although progress has been made for nucleons, in the case of $\bar{\theta}$, using lattice simulations [16]. An alternative is to use a low-energy effective field theory (EFT) of QCD, chiral perturbation theory (ChPT) [17, 18] (for a review, see for example Ref. [19]). In this case, we can describe hadronic and nuclear observables in a controlled expansion with minimal dynamical assumptions, where the symmetries of QCD—in particular the chiral $SU_L(2) \times SU_R(2)$ symmetry for two quark flavors—are respected order by order. While the simplest T -violating (TV) interactions have been known for a long time [20, 21, 22, 23, 24], a comprehensive analysis—similar to the well-known T -conserving (TC) sector—of the TV chiral Lagrangian from the $\bar{\theta}$ term [25] and the dimension-6 sources [26] has only been performed recently.

In the case of the nucleon EDM, one finds that, for T violation from the $\bar{\theta}$ term, the leading contributions come from the pion cloud, where the pion couples to the nucleon via a non-derivative P - and T -odd interaction, and from shorter-range interactions. The former is purely isovector, and provides an estimate of the EDM: the characteristic $\ln m_\pi$, with m_π the pion mass, is not expected to be canceled by short-range contributions and thus provides the bound on $\bar{\theta}$ mentioned above [20, 21, 23]. One can extend the calculation to the full electric dipole form factor (EDFF) as well [23], where in leading orders the radius, a contribution to the nucleon SM, is predicted [22]. However, because of two possible short-range structures, isoscalar and isovector, even measurements of both neutron and proton EDMs would

be insufficient to determine the three unknown parameters that appear at leading order.

When dimension-6 sources are included in the picture, one finds that the qCEDM generates a nucleon EDFF that is not distinguishable from the one stemming from $\bar{\theta}$ [24]. Furthermore, while the momentum dependence of the EDFF is qualitatively different if the qEDM or the gCEDM, rather than $\bar{\theta}$ or the qCEDM, are the dominant sources of T violation, a measurement of the neutron and proton EDMs alone can be fitted equally well by any of these sources. It is clear, then, that to pinpoint the dominant mechanism(s) of T violation at high energy, more observables are needed, and nuclear EDMs are natural candidates.

Nuclear EDMs and other moments receive various contributions. There are, of course, contributions from the individual nucleons' EDMs. In the deuteron the isovector component cancels, while in ^3He one can expect a cancellation between the contributions of the two nearly anti-aligned protons. Thus, nuclear EDMs, in particular the deuteron's [27, 28], are sensitive to a different combination of hadronic TV parameters than the neutron EDM. However, these one-nucleon contributions are modified from their "in-vacuum" counterparts because the nucleons are not free but bound in the nucleus. There are many-nucleon effects that are TV. First, the TV component of the pion cloud can generate a TV pion-exchange interaction among nucleons, and no symmetry forbids interactions of shorter range, either. These TV nuclear forces will mix-in components of the nuclear wave function that do not appear in the absence of TV. It is a source of polarization effects for the entire nucleus. Second, there may be multi-nucleon contributions to the TV coupling of the photon; such TV currents can be generated by either pion exchange or shorter-range dynamics.

TV one-pion exchange (OPE) has long been recognized as an important component of the TV two-nucleon (NN) potential, and expressed [29, 30] in terms of three non-derivative pion-nucleon couplings [31], associated with isospin $I = 0, 1, 2$. So far, the analysis of TV nuclear effects has been based on tree-level potentials where OPE is sometimes supplemented by the single exchange of heavier mesons, the eta [32], rho [33], and omega [33] being most popular. Allowing sufficiently many couplings of these mesons to nucleons one can produce [34] the most general short-range TV NN local interaction with one derivative [35]. This is the TV analog of the DDH approach [36] for nuclear TC P violation (PV).

The contributions from such potentials to the deuteron and ^3He EDMs have been calculated in the literature under various assumptions. OPE from the $I = 2$ TV pion-nucleon coupling does not contribute to the NN system at tree level. It was noticed early on [37] that OPE from the $I = 0$ TV pion-nucleon coupling does not contribute to the deuteron EDM, either, but it does for ^3He , where it was estimated with a phenomenological strong-interaction potential [38]. The deuteron EDM that arises from an $I = 1$ TV exchange of either pion- or shorter-range, together with a separable strong-interaction potential, was calculated in Ref. [37]. The effects of OPE on the deuteron EDM and MQM were calculated using both zero-range and phenomenological strong-interaction potentials in Ref. [39]. More recent calculations of the deuteron EDM and MQM [34] and of the ^3He EDM [40] have considered other TV contributions besides those from the TV potential, and used more modern, "realistic" strong-interaction potentials. Meson-exchange currents were found small in the deuteron [34], and neglected in ^3He [40]. The TV-potential contributions are consistent with earlier results; they are dominated by OPE from the $I = 1$ pion-nucleon coupling in the case of the deuteron [34], and from all three pion-nucleon couplings in the case of ^3He [40].

TV moments of heavier nuclei are more difficult to calculate. It has been argued [29] that the TV potential can lead to an enhancement over the nucleon EDM thanks to the near-degeneracy of levels of opposite parity, while meson-exchange currents are comparatively small. The size of the effect can be estimated through the single-particle potential obtained by averaging the NN potential over a closed nuclear core. The OPE from the $I = 0, 2$ pion-nucleon couplings are proportional to the nuclear I_3 , $(N - Z)/A$ [29, 30, 41], while the OPE from the $I = 1$ coupling does not have such a suppressing factor [30, 41]. It has also been found that the matrix elements from the rho and omega are small compared to the $I = 1$ pion contribution [33]. EDMs and MQMs (for example from $I = 0$ OPE [29]) and SMs [42] of several interesting nuclei have been estimated. A sample of recent SM calculations can be found in Refs. [7, 43].

There are, of course, other nuclear tests of TV, see for example Ref. [44]. The most promising for

effects of the TV nuclear interaction seems to be neutron scattering [45]. On the proton [46] and deuteron [47], TV neutron scattering is again dominated by OPE, but sensitive mostly to the $I = 0, 2$ and $I = 0, 1$ couplings, respectively. For heavy nuclei, one can again obtain estimates using the single-particle potential [30, 44].

For consistency, we would like to describe nuclear TV observables in the same framework used for the calculation of the nucleon EDM. The non-analytic behavior of the nucleon EDM in m_π and the dominance of OPE in nuclear observables point to the need of a framework that can account for both effects simultaneously, with chiral symmetry playing a central role. In fact, different sources of T violation have different transformation properties under chiral symmetry. As a consequence, the relative importance of various pion-nucleon and short-range interactions is not the same for all sources. Here we use the chiral Lagrangian built in Refs. [25, 26], where TV interactions stemming from the $\bar{\theta}$ term and the dimension-6 sources were constructed and ordered according to the same power counting used to order TC interactions in ChPT.

In addition to consistency between one- and few-nucleon TV interactions, nuclear TV also requires consistency between TV and TC forces, in order there to be no mismatch in the off-shell behaviors of the various ingredients. Of course, off-shell effects are dependent on the choice of fields, while physical quantities are not, provided the same choice of fields has been made throughout the calculation. As far as TV nuclear interactions are concerned, phenomenological TC models bring additional uncertainties, such as the choice of zero-range or finite-range interactions and the role of heavy mesons. On the other hand, ChPT has been extended to multi-nucleon systems [48], leading to the derivation of TC nuclear forces and currents. This opens up the possibility of describing all necessary ingredients in a single framework.

The goal of this paper is to provide the first step in the extension of TV interactions in the EFT to the multi-nucleon sector where OPE is treated non-perturbatively. Some of us have recently looked at the deuteron's PV, TV electromagnetic moments in an EFT where pions are treated in perturbation theory [28]. In this case, the size of uncertainties is set by the relatively low scale where OPE becomes significant. Treating OPE non-perturbatively extends the EFT to higher momenta and improves convergence. The TV nuclear potential is the most important ingredient in this extension, and here we derive it for the most important TV sources. This is the TV potential to be used, for example, with the TC, parity-conserving (PC) potentials from Refs. [49, 50, 51, 52, 53, 54, 55]. The construction here is similar to that of the TC PV potential [56, 57, 58], which extends the EFT from the TC, PV one-nucleon sector [59] to multi-nucleon systems. Such a framework provides an alternative to the DDH approach [36], allowing for a model-independent analysis of nuclear TC PV phenomena [60, 61]. Our present TV PV EFT framework stands in respect to previous approaches like this TC PV EFT framework with respect to the DDH approach.

As we are going to see, the form of the TV potential at a given order in the chiral expansion depends on the source. For the dimension-6 sources, all non-derivative pion-nucleon couplings appear at leading order, although these sources differ in the relative strength of the $I = 2$ pion-nucleon coupling and short-range interactions. For these sources, the leading-order potential is sufficient for most applications we envision. The situation is different for the $\bar{\theta}$ term: only the $I = 0$ pion-nucleon coupling, which is suppressed in some cases of interest, appears at leading order. For this source, we thus derive the potential up to subleading order. We show that new elements appear with respect to phenomenological treatments, such as two-pion exchange (TPE) at the same level as short-range interactions representing heavier-meson exchange. This richness is a blessing, as it potentially reveals the TV source [24, 28].

The rest of the paper is organized as follows. In the next section, Sect. 2, we present a summary of basic ChPT ideas and give the TC and TV chiral Lagrangians needed in the following sections. For processes involving momenta below $M_{nuc} \sim 100$ MeV, pion degrees of freedom can be integrated out and the dominant TV contact interactions (the leading-order TV potential in the so-called pionless EFT) are obtained in Sect. 3. The nuclear potential in ChPT, which should apply beyond M_{nuc} , is then presented in momentum (Sect. 4) and coordinate (Sect. 5) spaces. (We relegate details of the Fourier transformation to the Appendix.) In Sect. 6 we discuss the size of different components of the potential and compare them with phenomenological forms. We draw our conclusions in Sect. 7.

2 Chiral Perturbation Theory

QCD is characterized by an intrinsic mass scale $M_{QCD} \sim 1$ GeV. At momenta Q comparable to the pion mass, $Q \sim m_\pi \ll M_{QCD}$, interactions among nucleons and pions are described by the most general Lagrangian that involves these degrees of freedom and that has the same symmetries as QCD. A particularly important role at low energy is played by the approximate symmetry of QCD under the chiral group $SU_L(2) \times SU_R(2) \sim SO(4)$. Since it is not manifest in the spectrum, which instead exhibits an approximate isospin symmetry, chiral symmetry must be spontaneously broken down to the isospin subgroup $SU_{L+R}(2) \sim SO(3)$. The corresponding Goldstone bosons can be identified with the pions, which provide a non-linear realization of chiral symmetry.

Chiral symmetry and its spontaneous breaking strongly constrain the form of the interactions among nucleons and pions. In particular, in the limit of vanishing quark masses and charges, when chiral symmetry is exact, pion interactions proceed through a covariant derivative, which in stereographic coordinates $\vec{\pi}$ for the pions is [62]

$$D_\mu \vec{\pi} = D^{-1} \partial_\mu \vec{\pi} \quad (1)$$

with

$$D = 1 + \vec{\pi}^2 / F_\pi^2 \quad (2)$$

and $F_\pi \simeq 186$ MeV the pion decay constant. One can also construct the covariant derivative of this covariant derivative,

$$\mathcal{D}_\nu D_\mu \vec{\pi} = \partial_\nu D_\mu \vec{\pi} + \frac{2}{F_\pi^2} (\vec{\pi} \cdot D_\nu \vec{\pi} \cdot D_\mu \vec{\pi} - D_\nu \vec{\pi} \cdot \vec{\pi} \cdot D_\mu \vec{\pi}), \quad (3)$$

and so on. Nucleons are described by an isospin-1/2 field N , and we can define a nucleon covariant derivative

$$\mathcal{D}_\mu N = \left(\partial_\mu + \frac{i}{F_\pi^2} \vec{\tau} \cdot (\vec{\pi} \times D_\mu \vec{\pi}) \right) N, \quad (4)$$

where τ_i , $i = 1, 2, 3$, are the Pauli matrices in isospin space. We also define \mathcal{D}^\dagger through $\bar{N} \mathcal{D}^\dagger = \overline{\mathcal{D} N}$, and use the shorthand notation

$$\mathcal{D}_\pm^\mu \equiv \mathcal{D}^\mu \pm \mathcal{D}^{\dagger\mu}, \quad \mathcal{D}_\pm^\mu \mathcal{D}_\pm^\nu \equiv \mathcal{D}^\mu \mathcal{D}^\nu + \mathcal{D}^{\dagger\nu} \mathcal{D}^{\dagger\mu} \pm \mathcal{D}^{\dagger\mu} \mathcal{D}^\nu \pm \mathcal{D}^{\dagger\nu} \mathcal{D}^\mu \quad (5)$$

and

$$\tau_i \mathcal{D}_\pm^\mu \equiv \tau_i \mathcal{D}^\mu \pm \mathcal{D}^{\dagger\mu} \tau_i, \quad \tau_i \mathcal{D}_\pm^\mu \mathcal{D}_\pm^\nu \equiv \tau_i \mathcal{D}^\mu \mathcal{D}^\nu + \mathcal{D}^{\dagger\nu} \mathcal{D}^{\dagger\mu} \tau_i \pm \mathcal{D}^{\dagger\mu} \tau_i \mathcal{D}^\nu \pm \mathcal{D}^{\dagger\nu} \tau_i \mathcal{D}^\mu. \quad (6)$$

When acting on a nucleon bilinear of non-zero isospin, for example $\mathcal{D}_\mu (\bar{N} \vec{\tau} N)$, the covariant derivative is meant to be in the adjoint representation, that is, the isospin matrix in Eq. (4) should be replaced by $(t^j)_{ik} = i\epsilon^{ijk}$.

At $Q \sim m_\pi \ll m_N$, the nucleon mass, nucleons are essentially non-relativistic; as such the only coordinate with which their fields vary rapidly is $v \cdot x$, where v is the nucleon velocity, $v_\mu = (1, \vec{0})$ in the nucleon rest frame. It is convenient therefore to use a heavy-nucleon field from which this fast variation has been removed [63]. This simplifies the gamma-matrix algebra, leaving only the spin operator S^μ , where $S^\mu = (0, \vec{\sigma}/2)$ in the nucleon rest frame. Below we use the subscript \perp to denote the component of a four-vector perpendicular to the velocity, for example

$$\mathcal{D}_{\mu\perp} \equiv \mathcal{D}_\mu - v_\mu v \cdot \mathcal{D}. \quad (7)$$

Baryon states above the nucleon, such as the delta isobar, can be included in EFT along similar lines, but for simplicity we do not include them here.

The ChPT Lagrangian in the chiral limit includes all the interactions made out of $D_\mu \vec{\pi}$, N and their covariant derivatives that are chiral invariant. Chiral symmetry is explicitly broken, however, which introduces pion interactions that might not include derivatives, but are proportional to powers of the

symmetry-breaking parameters. Since the explicit breaking of chiral symmetry is small, chiral-symmetry-breaking operators can be systematically included as a perturbation on the chiral-invariant Lagrangian. Their forms are also not arbitrary, being instead determined by the chiral transformation properties of their progenitors in the QCD Lagrangian. The construction of chiral-symmetry-breaking operators from quark masses and “hard” electromagnetic interactions (those from photons with momenta beyond the EFT regime) is extensively treated in Refs. [62, 64]. “Soft” interactions via an explicit photon field A_μ appear in gauge-covariant derivatives,

$$(D_\mu \pi_a) \rightarrow \frac{1}{D} (\partial_\mu \delta_{ab} - e A_\mu \varepsilon_{3ab}) \pi_b, \quad (8)$$

$$\mathcal{D}_\mu N \rightarrow \left[\partial_\mu + \frac{i}{F_\pi^2} \vec{\tau} \cdot (\vec{\pi} \times D_\mu \vec{\pi}) - i e A_\mu \frac{1 + \tau_3}{2} \right] N, \quad (9)$$

where e is the proton electric charge, and in gauge-invariant interactions built from the photon field strength

$$F_{\mu\nu} = \partial_\mu A_\nu - \partial_\nu A_\mu. \quad (10)$$

Approximate chiral symmetry, together with the heavy-baryon formalism, allows us to systematically expand observables in the mesonic and one-nucleon sectors in powers of Q/M_{QCD} , where Q is the typical momentum of the process under consideration. The ChPT Lagrangian contains an infinite number of terms, which can be organized using an integer “chiral index” Δ and the number f of fermion fields [17, 62]:

$$\mathcal{L} = \sum_{\Delta=0}^{\infty} \sum_f \mathcal{L}_f^{(\Delta)}, \quad (11)$$

where $\Delta = d + f/2 - 2 \geq 0$, with d the number of derivatives, powers of the pion mass or of the electric charge. For processes with at most one nucleon, $A = 0, 1$, all momenta and energies are typically $\sim Q$. The contribution of a diagram to the amplitude T can then be estimated by

$$T \propto Q^\nu \mathcal{F}(Q/\mu), \quad (12)$$

where \mathcal{F} is a calculable function, μ is the renormalization scale, and the counting index ν is

$$\nu = 4 - 2C - A + 2L + \sum_i \Delta_i. \quad (13)$$

Here, $C = 1$ and L are respectively the number of connected pieces and loops in the diagrams, and i counts the number of insertions of vertices from $\mathcal{L}_f^{(\Delta)}$. From Eq. (13) it is apparent that diagrams with increasingly higher number of loops and non-vanishing-index interactions are increasingly suppressed, leading to a perturbative expansion. Assigning to loops a characteristic factor $Q^2/(4\pi)^2$ and using naive dimensional analysis [17, 65, 9] to estimate the EFT parameters, the suppression scale is $M_{QCD} \sim 2\pi F_\pi$. Note that in this sector of the theory nucleon recoil is a subleading effect: the nucleon is nearly static.

The ChPT power counting formula (13) cannot directly be applied to processes with $A \geq 2$ [66, 48]. Indeed, in diagrams in which the intermediate state consists purely of propagating nucleons—which are called “reducible”—the contour of integration for integrals over the 0th components of loop momenta cannot be deformed in way to avoid the poles of the nucleon propagators, thus picking up energies $\sim Q^2/m_N$ from nucleon recoil, no longer a subleading effect, rather than $\sim Q$. There is also an extra factor of 4π . These diagrams are therefore enhanced by factors of $4\pi m_N/Q$ with respect to the ChPT power counting that assigns $Q^2/(4\pi)^2$ to a loop, and the need to resum them leads to the appearance of shallow bound states in systems with two or more nucleons, nuclei. Diagrams whose intermediate states contain interacting nucleons and pions—“irreducible”—do not suffer from this infrared enhancement, and in them nucleon recoil remains a small effect. Reducible diagrams are thus obtained by patching together irreducible diagrams with intermediate states consisting of A free-nucleon propagators. Calling V the sum of all irreducible diagrams, the amplitude can be written schematically as

$$T = V + V G_0 V + V G_0 V G_0 V + \dots = V + V G_0 T, \quad (14)$$

where G_0 is the free-nucleon, non-relativistic Green's function. Equation (14) is just the Lippmann-Schwinger equation, which is formally equivalent to a Schrödinger equation with a potential V .

Naive dimensional analysis suggests [66] that irreducible diagrams follow the ChPT power counting rule (13) with $C \geq 1$. While this is true for pion-exchange diagrams, the situation is more complicated for contact interactions. In fact, it can be shown that the iteration of the singular one-pion exchange requires for renormalization at the same order a finite number of $f = 4$ interactions, some of which are less suppressed than expected on the basis of naive dimensional analysis [67, 68]. On the other hand, corrections, which should be perturbative, are expected to still conform to dimensional analysis [69, 70]. Since the TV potential is very small, it should be amenable to an expansion in powers of Q/M_{QCD} , with different contributions organized according to their chiral index ν , or, equivalently, according to the number of inverse powers of M_{QCD} .

In Sect. 4 we compute the TV nuclear potential, in the case of the QCD $\bar{\theta}$ term up to order $\nu = 3$, which means up to $\mathcal{O}(Q^2/M_{QCD}^2)$ with respect to the leading piece. Such a calculation requires the knowledge of the TC and TV ChPT Lagrangians up to $\Delta = 2$ and $\Delta = 3$, respectively. In the remainder of this section we present the relevant interactions. Throughout, we use nucleon field redefinitions to eliminate nucleon time derivatives from subleading interactions.

2.1 T -Conserving Chiral Lagrangian

The calculation of the TV potential in ChPT requires certain TC interactions with $f = 0, 2$, which we list here. (A more complete list can be found in the literature, for example Refs. [19, 48, 71].) These interactions stem from the quark (color-gauged) kinetic and mass terms in the QCD Lagrangian.

The leading TC chiral Lagrangian has chiral index $\Delta = 0$ and is given by

$$\mathcal{L}_{f \leq 2, T}^{(0)} = \frac{1}{2} D_\mu \vec{\pi} \cdot D^\mu \vec{\pi} - \frac{m_\pi^2}{2D} \vec{\pi}^2 + \bar{N} i v \cdot \mathcal{D} N - \frac{2g_A}{F_\pi} D_\mu \vec{\pi} \cdot \bar{N} \vec{\tau} S^\mu N, \quad (15)$$

where g_A is the pion-nucleon axial coupling, $g_A \simeq 1.27$. The pion mass term originates in explicit chiral-symmetry breaking by the average quark mass $\bar{m} = (m_u + m_d)/2$ and, by naive dimensional analysis, $m_\pi^2 = \mathcal{O}(\bar{m} M_{QCD})$. Neglecting for the moment isospin-breaking operators, at chiral order $\Delta = 1$ the relevant Lagrangian consists of

$$\mathcal{L}_{f \leq 2, TI}^{(1)} = -\frac{1}{2m_N} \bar{N} \mathcal{D}_\perp^2 N + \frac{g_A}{F_\pi m_N} (i v \cdot D \vec{\pi}) \cdot \bar{N} \vec{\tau} S \cdot \mathcal{D}_- N + \Delta m_N \left(1 - \frac{2\vec{\pi}^2}{F_\pi^2 D} \right) \bar{N} N. \quad (16)$$

Here the first two terms are the nucleon kinetic energy and a relativistic correction to the pion-nucleon coupling, the coefficients of both operators being fixed by Galilean invariance. The third term is the nucleon sigma term with a coefficient $\Delta m_N = \mathcal{O}(m_\pi^2/M_{QCD})$. At the next chiral order, $\Delta = 2$,

$$\begin{aligned} \mathcal{L}_{f \leq 2, TI}^{(2)} = & -\frac{\Delta m_\pi^2}{2D^2} \vec{\pi}^2 + \frac{g_A}{4F_\pi m_N^2} D_\mu \vec{\pi} \cdot \bar{N} \vec{\tau} \left(S^\mu \mathcal{D}_{\perp, -}^2 - \mathcal{D}_{\perp, -}^\mu S \cdot \mathcal{D}_{\perp, -} \right) N \\ & - \frac{2g_A}{F_\pi} \left[c_A \mathcal{D}_\perp^2 D_\mu \vec{\pi} - d_A \left(1 - \frac{2\vec{\pi}^2}{F_\pi^2 D} \right) D_\mu \vec{\pi} \right] \cdot \bar{N} \vec{\tau} S^\mu N. \end{aligned} \quad (17)$$

The first term is a correction to the pion mass, $\Delta m_\pi^2 = \mathcal{O}(m_\pi^4/M_{QCD}^2)$. The second term represents further relativistic corrections to the g_A term in Eq. (15). The constraints imposed by Lorentz invariance on Eqs. (16) and (17) agree with the results of Ref. [71], once a field redefinition is used to eliminate time derivatives acting on the nucleon field from the subleading $\Delta = 1$ and $\Delta = 2$ Lagrangians. The operator with coefficient $c_A = \mathcal{O}(1/M_{QCD}^2)$ in Eq. (17) is a contribution to the square radius of the pion-nucleon form factor, while $d_A = \mathcal{O}(m_\pi^2/M_{QCD}^2)$ is a chiral-symmetry-breaking correction to g_A [51], which provide the so-called Goldberger-Treiman discrepancy.

Isospin-breaking operators in the chiral Lagrangian [64] stem from the quark mass difference $m_d - m_u = 2\bar{m}\varepsilon$ and from quark coupling to photons through the fine-structure constant $\alpha_{\text{em}} = e^2/4\pi$. Here,

for simplicity, we count $\varepsilon \sim 1/3$ as $\mathcal{O}(1)$ and $\alpha_{\text{em}}/4\pi$ as $\mathcal{O}(m_\pi^3/M_{QCD}^3)$, since numerically $\alpha_{\text{em}}/4\pi \sim \varepsilon m_\pi^3/(2\pi F_\pi)^3$. Isospin-violating terms first contribute to the $\Delta = 1$ Lagrangian,

$$\mathcal{L}_{f \leq 2, TI}^{(1)} = -\frac{\check{\delta} m_\pi^2}{2D^2} (\vec{\pi}^2 - \pi_3^2) + \frac{\delta m_N}{2} \bar{N} \left(\tau_3 - \frac{2\pi_3}{F_\pi^2 D} \vec{\pi} \cdot \vec{\tau} \right) N, \quad (18)$$

while at order $\Delta = 2$,

$$\mathcal{L}_{f \leq 2, TI}^{(2)} = -\frac{\delta m_\pi^2}{2D^2} \pi_3^2 + \frac{\check{\delta} m_N}{2} \bar{N} \left[\tau_3 + \frac{2}{F_\pi^2 D} (\pi_3 \vec{\pi} \cdot \vec{\tau} - \vec{\pi}^2 \tau_3) \right] N + \frac{\beta_1}{F_\pi} \left(D_\mu \pi_3 - \frac{2\pi_3}{F_\pi^2 D} \vec{\pi} \cdot D_\mu \vec{\pi} \right) \bar{N} S^\mu N. \quad (19)$$

Here $\check{\delta} m_\pi^2 = \mathcal{O}(\alpha_{\text{em}} M_{QCD}^2/4\pi)$ is the leading electromagnetic contribution to the pion mass splitting, while the quark-mass-difference contribution, $\delta m_\pi^2 = \mathcal{O}(\varepsilon^2 m_\pi^4/M_{QCD}^2)$, is smaller by a power of $\varepsilon m_\pi/M_{QCD}$. The pion mass splitting, $m_{\pi^\pm}^2 - m_{\pi^0}^2 = \check{\delta} m_\pi^2 - \delta m_\pi^2 = (35.5 \text{ MeV})^2$ [72], is dominated by the electromagnetic contribution. The nucleon mass splitting, $m_n - m_p = \delta m_N + \check{\delta} m_N = 1.29 \text{ MeV}$ [72] also receives contributions from electromagnetism and from the quark masses. In this case, the quark-mass contribution δm_N is expected to be the largest. By dimensional analysis $\delta m_N = \mathcal{O}(\varepsilon m_\pi^2/M_{QCD})$, and lattice simulations estimate it to be $\delta m_N = 2.26 \pm 0.57 \pm 0.42 \pm 0.10 \text{ MeV}$ [73], which is in agreement with an extraction from charge-symmetry breaking in the $pn \rightarrow d\pi^0$ reaction [74]. The electromagnetic contribution is $\check{\delta} m_N = \mathcal{O}(\alpha_{\text{em}} M_{QCD}/4\pi)$, that is, $\mathcal{O}(\varepsilon m_\pi^3/M_{QCD}^2)$ and about the 20% of δm_N . Using the Cottingham sum rule, $\check{\delta} m_N = -(0.76 \pm 0.30) \text{ MeV}$ [75], which is consistent with dimensional analysis. The operator with coefficient $\beta_1 = \mathcal{O}(\varepsilon m_\pi^2/M_{QCD}^2)$ is an isospin-violating pion-nucleon coupling. At present there are only bounds on β_1 from isospin violation in nucleon-nucleon scattering. For example, a phase-shift analysis of two-nucleon data gives $\beta_1 = (0 \pm 9) \cdot 10^{-3}$ [51, 52], which is comparable to estimates of β_1 from π - η mixing.

For the solution of the Lippmann-Schwinger equation, it is convenient to eliminate the nucleon mass difference $m_n - m_p$ from the nucleon propagator and from asymptotic states. This result can be accomplished through a field redefinition, defined in Ref. [54]. After the field redefinition, Eqs. (18) and (19) become

$$\begin{aligned} \mathcal{L}_{f \leq 2, TI}^{(1,2)} = & -\frac{1}{2D^2} (\check{\delta} m_\pi^2 - \delta m_N^2) (\vec{\pi}^2 - \pi_3^2) - \frac{\delta m_\pi^2}{2D^2} \pi_3^2 - (\delta m_N + \check{\delta} m_N) (\vec{\pi} \times v \cdot D \vec{\pi})_3 \\ & + \frac{g_A \delta m_N}{F_\pi m_N} i \varepsilon_{3ab} \pi_a \bar{N} \tau_b S \cdot D_- N + \frac{\beta_1}{F_\pi} \left(D_\mu \pi_3 - \frac{2\pi_3}{F_\pi^2 D} \vec{\pi} \cdot D_\mu \vec{\pi} \right) \bar{N} S^\mu N. \end{aligned} \quad (20)$$

We will incorporate isospin-breaking effects in the potential using the Lagrangian (20).

2.2 T-Violating Chiral Lagrangian From $\bar{\theta}$

The lowest-dimension TV operator that can be added to the TC QCD Lagrangian is the dimension-4 $\bar{\theta}$ term. With an appropriate choice of the quark fields $q = (u, d)^T$, the $\bar{\theta}$ term can be expressed as a complex mass term [76],

$$\mathcal{L}_{T4} = m_\star \bar{\theta} \bar{q} i \gamma_5 q, \quad (21)$$

where $m_\star = m_u m_d / (m_u + m_d) = \mathcal{O}(m_\pi^2/M_{QCD})$ and $\bar{\theta}$ is the QCD vacuum angle, here already assumed to be small as indicated by the bound on the neutron EDM, $\bar{\theta} \lesssim 10^{-10}$. The $\bar{\theta}$ term transforms under chiral symmetry as the fourth component of an $SO(4)$ vector $P = (\bar{q} \vec{\tau} q, \bar{q} i \gamma_5 q)$, whose third component is responsible for quark-mass isospin violation [64]. TV from the $\bar{\theta}$ term and isospin violation from the quark mass difference are therefore intrinsically linked; this link appears in certain relations [20, 25] between the coefficients of TV and isospin-breaking operators in ChPT through a coefficient $\rho = (1 - \varepsilon^2) \bar{\theta} / 2\varepsilon$.

The pion-nucleon TV Lagrangian from the QCD $\bar{\theta}$ term was constructed in Ref. [25]. The leading $f \leq 2$ TV interaction generated by the $\bar{\theta}$ term appears at $\Delta = 1$ and consists of an isoscalar pion-nucleon

coupling,

$$\mathcal{L}_{f=2,T^4}^{(1)} = -\frac{\bar{g}_0}{F_\pi D} \vec{\pi} \cdot \bar{N} \vec{\tau} N. \quad (22)$$

The relation to isospin-breaking operators implies that \bar{g}_0 can be expressed in terms of the quark-mass contribution to the nucleon mass difference, $\bar{g}_0 = \rho \delta m_N = \mathcal{O}(\bar{\theta} m_\pi^2 / M_{QCD})$. Increasing the chiral index by one, we find a single term,

$$\mathcal{L}_{f=2,T^4}^{(2)} = -\frac{2\bar{h}_0}{F_\pi^2 D} \vec{\pi} \cdot D_\mu \vec{\pi} \bar{N} S^\mu N, \quad (23)$$

where \bar{h}_0 is an isoscalar two-pion-nucleon coupling, which is related to the coefficient β_1 in Eq. (20) by $\bar{h}_0 = \rho \beta_1 = \mathcal{O}(\bar{\theta} m_\pi^2 / M_{QCD}^2)$. The $\Delta = 3$ operators relevant to the calculation of the TV potential at order $\nu = 3$ are

$$\begin{aligned} \mathcal{L}_{f=2,T^4}^{(3)} = & -\frac{1}{F_\pi} \left(\frac{\bar{g}_1}{D} - 2\bar{g}_0 \frac{\Delta m_N}{\delta m_N} \frac{\delta m_\pi^2}{m_\pi^2} \right) \left(1 - \frac{2\vec{\pi}^2}{F_\pi^2 D} \right) \pi_3 \bar{N} N \\ & - \frac{1}{F_\pi} \left(\frac{\Delta \bar{g}_0}{D} - \bar{g}_0 \frac{\delta m_\pi^2}{m_\pi^2} \right) \left(1 - \frac{2\vec{\pi}^2}{F_\pi^2 D} \right) \vec{\pi} \cdot \bar{N} \vec{\tau} N + \frac{\bar{\eta}}{2F_\pi} \left(1 - \frac{2\vec{\pi}^2}{F_\pi^2 D} \right) (\mathcal{D}_\mu \perp D_\mu^\perp \vec{\pi}) \cdot \bar{N} \vec{\tau} N, \\ & + \frac{\bar{g}_0}{8m_N^2 F_\pi D} \left\{ \vec{\pi} \cdot \bar{N} \vec{\tau} \mathcal{D}_\perp^2 N + 2 \left(1 - \frac{\vec{\pi}^2}{F_\pi^2} \right) D_\nu \vec{\pi} \cdot \bar{N} \vec{\tau} [S^\mu, S^\nu] \mathcal{D}_\mu N \right\}, \end{aligned} \quad (24)$$

where once again we eliminated operators containing nucleon time derivatives and neglected multi-pion operators. Equation (24) is obtained after rotating away the subleading pion tadpole operator $-(\bar{g}_0 \delta m_\pi^2 / 2 \delta m_N) \pi_3$ from the mesonic TV Lagrangian, as detailed in Ref. [25]. The first operator in Eq. (24) is the most important contribution of the θ term to the isospin-breaking TV non-derivative coupling $\pi_3 \bar{N} N$. Its coefficient is of $\mathcal{O}(\theta \varepsilon m_\pi^4 / M_{QCD}^3)$ and is suppressed by two powers of m_π / M_{QCD} with respect to \bar{g}_0 . The second term in Eq. (24) is basically a correction to \bar{g}_0 of the same order. Of the TV operators with two derivatives, $\bar{\eta} = \mathcal{O}(\theta m_\pi^2 / M_{QCD}^3)$ represents a contribution to the radius of the TV pion-nucleon form factor, while the remaining operators relevant at this order are relativistic corrections to the \bar{g}_0 term with coefficients fixed by Lorentz invariance. As in the case of the $\Delta = 1, 2$ TV Lagrangians, the TV coefficients in Eq. (24) are related to isospin-violating parameters in the $\Delta = 3$ TC Lagrangian, which are at present poorly determined (see discussion in Ref. [25]).

For the nuclear potential we will need in addition operators involving more nucleon fields, which are constructed in the same way as were the $f = 0, 2$ interactions in Ref. [25]. In the $f = 4$ sector of the theory, the first contribution to the Lagrangian comes at $\Delta = 2$,

$$\mathcal{L}_{f=4,T^4}^{(2)} = -\frac{1}{F_\pi D} \vec{\pi} \cdot (\bar{\gamma}_s \bar{N} \vec{\tau} N \bar{N} N + 4\bar{\gamma}_\sigma \bar{N} \vec{\tau} S_\mu N \bar{N} S^\mu N), \quad (25)$$

in terms of two TV parameters $\bar{\gamma}_{s,\sigma}$. Just as for $f \leq 2$, here too there is a link with isospin-violating operators, in this case

$$\mathcal{L}_{f=4,T^4}^{(2)} = \frac{\gamma_s}{2} \bar{N} \left(\tau_3 - \frac{2\pi_3}{F_\pi^2 D} \vec{\pi} \cdot \vec{\tau} \right) N \bar{N} N + 2\gamma_\sigma \bar{N} \left(\tau_3 - \frac{2\pi_3}{F_\pi^2 D} \vec{\pi} \cdot \vec{\tau} \right) S_\mu N \bar{N} S^\mu N, \quad (26)$$

which generate the dominant contributions to the short-range isospin-violating two-nucleon potential [64, 51]. The isospin-violating coefficients $\gamma_i = \mathcal{O}(\varepsilon m_\pi^2 / F_\pi^2 M_{QCD}^2)$ can be seen as low-energy remnants of ρ - ω mixing [51] and a_1 - f_1 mixing [77]. The TV parameters are related to them by $\bar{\gamma}_i = \rho \gamma_i = \mathcal{O}(\bar{\theta} m_\pi^2 / F_\pi^2 M_{QCD}^2)$. The operators in Eq. (25) are not relevant for the nuclear potential to the order we work, but contribute to the three-nucleon TV potential at next order.

The first operators relevant to the calculation of the TV two-nucleon potential are

$$\mathcal{L}_{f=4,T^4}^{(3)} = \left(1 - \frac{2\vec{\pi}^2}{F_\pi^2 D} \right) [\bar{C}_1 \bar{N} N \partial_\mu (\bar{N} S^\mu N) + \bar{C}_2 \bar{N} \vec{\tau} N \cdot \mathcal{D}_\mu (\bar{N} S^\mu \vec{\tau} N)], \quad (27)$$

where the \bar{C}_i are two new TV parameters. These interactions are related to isospin-breaking operators

$$\mathcal{L}_{f=4, TI}^{(3)} = \frac{2\pi_3}{F_\pi D} [C_1 \bar{N} N \partial_\mu (\bar{N} S^\mu N) + C_2 \bar{N} \vec{\tau} N \cdot \mathcal{D}_\mu (\bar{N} S^\mu \vec{\tau} N)] , \quad (28)$$

with coefficients $C_i = \mathcal{O}(\varepsilon m_\pi^2 / F_\pi^2 M_{QCD}^3)$. The TV parameters are $\bar{C}_i = \rho C_i = \mathcal{O}(\bar{\theta} m_\pi^2 / F_\pi^2 M_{QCD}^3)$ and, therefore, contribute to the TV potential at order $\nu = 3$. The coefficients C_i could in principle be determined from pion production in the two-nucleon system and/or from isospin-violating three-nucleon forces. However, even lower-order isospin-violating three-nucleon forces are very small [55], so prospects for extracting C_i from TC data are grim. As before, we do not write in Eq. (27) other interactions that contain more pion fields.

One can continue the construction of the TV Lagrangian not only to higher orders, but also to more nucleon fields. For any given f , the dominant TV terms are expected to be those without derivatives that transform like the fourth component P_4 , just as in Eq. (25). This type of term will involve an odd number of pions in addition to the f nucleon fields. It thus contributes at tree level only to $(f+2)/2$ -nucleon forces, or to absorption/production/scattering of pions on $f/2$ -nucleon systems. The first short-range $f/2$ -nucleon TV force comes from four-vectors P that involve one derivative, as in Eq. (27). Since nuclear forces tend to become less important as f increases (see, for example, Ref. [48]), it is unlikely that terms with $f \geq 6$ need to be constructed. The first $f = 6$ operators that contribute to the three-nucleon TV potential appear at next chiral order, $\Delta = 4$.

2.3 T -Violating Chiral Lagrangian From Dimension-6 Sources

The smallness of $\bar{\theta}$ leaves room for other sources of T violation in the strong interactions, which have their origin in an ultraviolet-complete theory at a high-energy scale, such as, for example, supersymmetric extensions of the Standard Model [11]. Well below the scale M_T characteristic of T violation, we expect TV effects to be captured by the lowest-dimension interactions among Standard Model fields that respect the theory's $SU_c(3) \times SU_L(2) \times U_Y(1)$ gauge symmetry. Just above M_{QCD} , strong interactions are described by the most general Lagrangian with Lorentz, and color and electromagnetic gauge invariance among the lightest quarks, gluons, and photons. The effectively dimension-6 TV terms at this scale can be written as [8, 9, 10, 11]

$$\begin{aligned} \mathcal{L}_{T6} = & -\frac{1}{2} \bar{q} (d_0 + d_3 \tau_3) \sigma^{\mu\nu} i \gamma^5 q F_{\mu\nu} - \frac{1}{2} \bar{q} (\tilde{d}_0 + \tilde{d}_3 \tau_3) \sigma^{\mu\nu} i \gamma^5 \lambda^a q G_{\mu\nu}^a \\ & + \frac{d_W}{6} \varepsilon^{\mu\nu\lambda\sigma} f^{abc} G_{\mu\rho}^a G_\nu^b G_{\lambda\sigma}^c + \frac{1}{4} \text{Im} \Sigma_1 (\bar{q} q \bar{q} i \gamma^5 q - \bar{q} \vec{\tau} q \cdot \bar{q} \vec{\tau} i \gamma^5 q) \\ & + \frac{1}{4} \text{Im} \Sigma_8 (\bar{q} \lambda^a q \bar{q} \lambda^a i \gamma^5 q - \bar{q} \lambda^a \vec{\tau} q \cdot \bar{q} \lambda^a \vec{\tau} i \gamma^5 q) , \end{aligned} \quad (29)$$

in terms of the photon and gluon field strengths $F_{\mu\nu}$ and $G_{\mu\nu}^a$, the standard products of gamma matrices γ^5 and $\sigma^{\mu\nu}$ in spin space, the totally antisymmetric symbol $\varepsilon^{\mu\nu\lambda\sigma}$, the Pauli matrix τ_i in isospin space, the Gell-Mann matrices λ^a in color space, and the associated Gell-Mann coefficients f^{abc} .

In Eq. (29) the first (second) term represents the isoscalar d_0 (\tilde{d}_0) and isovector d_3 (\tilde{d}_3) components of the qEDM (qCEDM). Although these interactions have canonical dimension 5, they originate just above the Standard Model scale M_W from dimension-6 operators [8] involving in addition the carrier of electroweak symmetry breaking, the Higgs field. They are thus proportional to the vacuum expectation value of the Higgs field, which we can trade for the ratio of the quark mass to Yukawa coupling, m_q/f_q . Writing the proportionality constant as $e\delta_q f_q/M_T^2$ ($4\pi\tilde{\delta}_q f_q/M_T^2$),

$$d_{0,3} \sim \mathcal{O} \left(e\delta_{0,3} \frac{\bar{m}}{M_T^2} \right) , \quad \tilde{d}_{0,3} \sim \mathcal{O} \left(4\pi\tilde{\delta}_{0,3} \frac{\bar{m}}{M_T^2} \right) , \quad (30)$$

in terms of the average light-quark mass \bar{m} and the dimensionless factors $\delta_{0,3}$ and $\tilde{\delta}_{0,3}$ representing typical values of δ_q and $\tilde{\delta}_q$. The third term in Eq. (29) [9] is the gCEDM, with coefficient

$$d_W \sim \mathcal{O}\left(\frac{4\pi w}{M_T^2}\right) \quad (31)$$

in terms of a dimensionless parameter w . The fourth and fifth operators [10, 11] are TV FQ operators, with coefficients

$$\text{Im}\Sigma_{1,8} = \mathcal{O}\left(\frac{(4\pi)^2 \sigma_{1,8}}{M_T^2}\right) \quad (32)$$

in terms of further dimensionless parameters $\sigma_{1,8}$. The sizes of $\delta_{0,3}$, $\tilde{\delta}_{0,3}$, w , and $\sigma_{1,8}$ depend on the exact mechanisms of electroweak and T breaking and on the running to the low energies where non-perturbative QCD effects take over. The minimal assumption is that they are $\mathcal{O}(1)$, $\mathcal{O}(g_s/4\pi)$, $\mathcal{O}((g_s/4\pi)^3)$, and $\mathcal{O}(1)$, respectively, with g_s the strong coupling constant. However they can be much smaller (when parameters encoding TV beyond the Standard Model are small) or much larger (since f_q is unnaturally small). For discussion and examples, see Refs. [4, 11].

The dimension-6 operators in Eq. (29) have different transformation properties under chiral symmetry. The isoscalar and isovector qEDM (qCEDM) transform, respectively, as the fourth and third components of two $SO(4)$ vectors V and W (\tilde{V} and \tilde{W}), with

$$V = \frac{1}{2} \begin{pmatrix} \bar{q}\sigma^{\mu\nu}\vec{\tau}q \\ i\bar{q}\sigma^{\mu\nu}\gamma^5 q \end{pmatrix} F_{\mu\nu}, \quad W = \frac{1}{2} \begin{pmatrix} -i\bar{q}\sigma^{\mu\nu}\gamma^5\vec{\tau}q \\ \bar{q}\sigma^{\mu\nu}q \end{pmatrix} F_{\mu\nu}, \quad (33)$$

and

$$\tilde{V} = \frac{1}{2} \begin{pmatrix} \bar{q}\sigma^{\mu\nu}\vec{\tau}\lambda^a q \\ i\bar{q}\sigma^{\mu\nu}\gamma^5\lambda^a q \end{pmatrix} G_{\mu\nu}^a, \quad \tilde{W} = \frac{1}{2} \begin{pmatrix} -i\bar{q}\sigma^{\mu\nu}\gamma^5\vec{\tau}\lambda^a q \\ \bar{q}\sigma^{\mu\nu}\lambda^a q \end{pmatrix} G_{\mu\nu}^a. \quad (34)$$

In contrast, the gCEDM and the two TV FQ operators $\Sigma_{1,8}$ are singlets of the chiral group, respectively

$$I_W = \frac{1}{6} \varepsilon^{\mu\nu\lambda\sigma} f^{abc} G_{\mu\rho}^a G_\nu^b G_{\lambda\sigma}^c \quad (35)$$

and

$$I_{qq1} = \frac{1}{4} (\bar{q}q \bar{q}i\gamma^5 q - \bar{q}\vec{\tau}q \cdot \bar{q}\vec{\tau}i\gamma^5 q), \quad (36)$$

$$I_{qq8} = \frac{1}{4} (\bar{q}\lambda^a q \bar{q}\lambda^a i\gamma^5 q - \bar{q}\lambda^a \vec{\tau}q \cdot \bar{q}\lambda^a \vec{\tau}i\gamma^5 q). \quad (37)$$

They do not break chiral symmetry.

The different chiral properties of various TV sources have profound implications for the form and relative importance of nucleon-pion and nucleon-nucleon TV couplings in the effective Lagrangian. Effective interactions are constructed to transform in the same way as the sources at quark/gluon level. Thus, \tilde{W}_3 leads to interactions proportional to $\tilde{\delta}_3$ that only appear from $\bar{\theta}$ in the tensor product between P_4 and P_3 from the quark-mass-difference term, and are thus proportional to $\varepsilon\bar{m}^2\bar{\theta}$ (for example, the \tilde{g}_1 term in Eq. (24)).

On the other hand, \tilde{V}_4 generates exactly the same interactions as P_4 , so $\tilde{\delta}_0$ and $\bar{\theta}$ contribute similarly to low-energy observables. For qEDM, hadronic interactions arise from integrating out at least one hard photon, which leads to further breaking of chiral symmetry in the form of tensor products of V and W with a antisymmetric chiral tensor [64]. The contributions of the qEDM to purely hadronic couplings, like pion-nucleon or nucleon-nucleon couplings, are suppressed by the electromagnetic coupling constant, $\alpha_{\text{em}}/4\pi \sim \varepsilon m_\pi^3/(2\pi F_\pi)^3$. electromagnetic currents. We do not explicitly construct the TV potential from the qEDM. Because they are chiral invariant, the gCEDM and the two TV FQ operators lead to

exactly the same effective interactions, although, of course, with different strengths. The interactions from gCEDM are the hadronic matrix elements of I_W (35) and are proportional to w in Eq. (31), while those from the TV FQ operators are the hadronic matrix elements of I_{qqi} in Eqs. (36) and (37) and are proportional to σ_i in Eq. (32). For simplicity of notation, in the following w denotes both w and $\sigma_{1,8}$,

$$\{w, \sigma_1, \sigma_8\} \rightarrow w. \quad (38)$$

For none of the dimension-6 sources there is an immediate, useful connection to TC operators as for $\bar{\theta}$.

The pion-nucleon Lagrangian from dimension-6 sources was constructed in detail in Ref. [26]. The only terms we need in the following belong to the lowest-order Lagrangian,

$$\begin{aligned} \mathcal{L}_{f=2,T6}^{(\Delta_\pi)} = & -\frac{\bar{g}_0}{F_\pi D} \vec{\pi} \cdot \bar{N} \vec{\tau} N - \frac{\bar{g}_1}{F_\pi D} \pi_3 \bar{N} N - \frac{\bar{g}_2}{F_\pi D} \pi_3 \bar{N} \left[\tau_3 + \frac{2}{F_\pi^2 D} (\pi_3 \vec{\pi} \cdot \vec{\tau} - \vec{\pi}^2 \tau_3) \right] N \\ & - \frac{\bar{v}_0}{F_\pi^2} (v \cdot D \vec{\pi} \times D_\mu \vec{\pi}) \cdot \bar{N} S^\mu \vec{\tau} N - \frac{\bar{v}_1}{F_\pi} \mathcal{D}_\perp \cdot D_\perp \vec{\pi} \cdot \bar{N} \vec{\tau} N. \end{aligned} \quad (39)$$

In this Lagrangian:

- For qCEDM, $\Delta_\pi = -1$. At this order the qCEDM contributes only to the non-derivative couplings \bar{g}_0 and \bar{g}_1 . In contrast to the $\bar{\theta}$ case (24), the elimination of the pion tadpoles induced by the isovector component \tilde{W}_3 of the qCEDM generates an interaction of exactly the same chiral form as other existing interactions, and for simplicity we absorb the tadpole contribution in the \bar{g}_i . Then $\bar{g}_0 = \mathcal{O}((\tilde{\delta}_0 + \varepsilon \tilde{\delta}_3) m_\pi^2 M_{QCD}/M_T^2)$ and $\bar{g}_1 = \mathcal{O}(\tilde{\delta}_3 m_\pi^2 M_{QCD}/M_T^2)$.
- For qEDM, $\Delta_\pi = 2$. At this order the qEDM contributes also to the non-derivative coupling \bar{g}_2 , which arises from the tensor product of W_3 with the antisymmetric chiral tensor generated by a hard photon. In this case, again after tadpole extermination, $\bar{g}_0 = \mathcal{O}(\alpha_{\text{em}}(\delta_0 + \delta_3)(1 + \varepsilon) m_\pi^2 M_{QCD}/4\pi M_T^2)$, $\bar{g}_1 = \mathcal{O}(\alpha_{\text{em}}(\delta_0 + \delta_3) m_\pi^2 M_{QCD}/4\pi M_T^2)$, and $\bar{g}_2 = \mathcal{O}(\alpha_{\text{em}} \delta_3 m_\pi^2 M_{QCD}/4\pi M_T^2)$.
- For chiral-invariant sources, $\Delta_\pi = -1$. It is not possible to construct chiral-invariant, TV pion-nucleon couplings with zero or one derivatives. The leading TV couplings then contain either two derivatives or one insertion of the quark mass, and the couplings $\bar{g}_{0,1}$ and $\bar{v}_{0,1}$ all appear at the same order. More precisely, after the elimination of the pion tadpole, we find $\bar{g}_0 = \mathcal{O}(w(1 + \varepsilon^2) m_\pi^2 M_{QCD}/M_T^2)$ and $\bar{g}_1 = \mathcal{O}(w \varepsilon m_\pi^2 M_{QCD}/M_T^2)$, while $\bar{v}_{0,1} = \mathcal{O}(w M_{QCD}/M_T^2)$.

In the case of qEDM, we need also the photon-nucleon TV interactions [24, 26]

$$\mathcal{L}_{f=2,T6}^{(1)} = 2\bar{N} \left[\bar{d}_0 \left(1 - \frac{2\vec{\pi}^2}{F_\pi^2 D} \right) + \bar{d}_1 \left(\tau_3 - \frac{2\pi_3}{F_\pi^2 D} \vec{\pi} \cdot \vec{\tau} \right) \right] S^\mu N v^\nu F_{\mu\nu}, \quad (40)$$

with $\bar{d}_{0,1} = \mathcal{O}(e \delta_{0,3} m_\pi^2 / M_T^2 M_{QCD})$ short-range contributions to the nucleon EDM.

The various dimension-6 sources lead to different interactions also in the $f \geq 4$ sectors. For the chiral-invariant sources, there are further leading-order interactions with $f = 4$,

$$\mathcal{L}_{f=4,T6}^{(-1)} = \bar{C}_1 \bar{N} N \partial_\mu (\bar{N} S^\mu N) + \bar{C}_2 \bar{N} \vec{\tau} N \cdot \mathcal{D}_\mu (\bar{N} \vec{\tau} S^\mu N), \quad (41)$$

with coefficients $\bar{C}_{1,2} = \mathcal{O}(w M_{QCD}/F_\pi^2 M_T^2)$. Note that because of different chiral-transformation properties, the form of Eq. (41) is different from the contact interactions stemming from $\bar{\theta}$, Eq. (27). For the remaining dimension-6 sources, the form of contact interactions can be different still. They appear from tensor products of symmetry-breaking operators and are subleading. The qCEDM and qEDM generate operators at chiral index $\Delta = \Delta_\pi + 1$, which have schematically the same form as Eq. (25), but a richer isospin structure. These operators do not contribute to the two-nucleon potential at tree level, but they

are relevant for three-nucleon forces just beyond the order we consider. Contributions from these sources to the two-nucleon potential are found at $\Delta = \Delta_\pi + 2$,

$$\begin{aligned}\mathcal{L}_{f=4,T6}^{(\Delta_\pi+2)} = & \left(1 - \frac{2\vec{\pi}^2}{F_\pi^2 D}\right) [\bar{C}_1 \bar{N} N \partial_\mu (\bar{N} S^\mu N) + \bar{C}_2 \bar{N} \vec{\tau} N \cdot \mathcal{D}_\mu (\bar{N} S^\mu \vec{\tau} N)] \\ & + \left(\delta_{3k} - \frac{2\pi_3}{F_\pi^2 D} \pi_k\right) [\bar{C}_3 \bar{N} \tau_k N \partial_\mu (\bar{N} S^\mu N) + \bar{C}_4 \bar{N} N \mathcal{D}_\mu (\bar{N} \tau_k S^\mu N)] \\ & + \left\{ \left(1 - \frac{2\vec{\pi}^2}{F_\pi^2 D}\right) [\bar{C}_5 \bar{N} \tau_l N \partial_\mu (\bar{N} S^\mu N) + \bar{C}_6 \bar{N} N \mathcal{D}_\mu (\bar{N} \tau_l S^\mu N)] \right. \\ & \left. + \bar{C}_7 \left(\delta_{3k} - \frac{2\pi_3}{F_\pi^2 D} \pi_k\right) \bar{N} \tau_k N \mathcal{D}_\mu (\bar{N} S^\mu \tau_l N) \right\} \left[\delta_{l3} + \frac{2}{F_\pi^2 D} (\pi_3 \pi_l - \vec{\pi}^2 \delta_{3l}) \right], \quad (42)\end{aligned}$$

where the \bar{C}_i are new coefficients. The qCEDM only contributes to $\bar{C}_{1,2,3,4}$ in lowest order, with $\bar{C}_{1,2} = \mathcal{O}((\tilde{\delta}_0 + \varepsilon \tilde{\delta}_3) m_\pi^2 / F_\pi^2 M_T^2 M_{QCD})$ and $\bar{C}_{3,4} = \mathcal{O}(\tilde{\delta}_3 m_\pi^2 / F_\pi^2 M_T^2 M_{QCD})$. The qEDM contributes also to $\bar{C}_{5,6,7}$, because of tensor products with the antisymmetric tensor generated by a hard photon, and we have $\bar{C}_{1,2} = \mathcal{O}(\alpha_{\text{em}}(\delta_0 + \delta_3)(1 + \varepsilon) m_\pi^2 / 4\pi F_\pi^2 M_T^2 M_{QCD})$, $\bar{C}_{3,4} = \mathcal{O}(\alpha_{\text{em}}(\delta_0 + \delta_3) m_\pi^2 / 4\pi F_\pi^2 M_T^2 M_{QCD})$, $\bar{C}_{5,6} = \mathcal{O}(\alpha_{\text{em}} \delta_0 m_\pi^2 / 4\pi F_\pi^2 M_T^2 M_{QCD})$, and $\bar{C}_7 = \mathcal{O}(\alpha_{\text{em}} \delta_3 m_\pi^2 / 4\pi F_\pi^2 M_T^2 M_{QCD})$. Comparing Eq. (42) to Eq. (27), we once again see that, differently from the $\bar{\theta}$ term, the qCEDM and qEDM generate TV and isospin-breaking operators of the same importance as isoscalar TV operators. The four-nucleon operators in Eq. (42) have, this time just like the $\bar{\theta}$ term, chiral index that is two units bigger than that of the leading pion-nucleon Lagrangian. As a consequence, short-range contributions to the two-nucleon potential from these sources arise only at next-to-next-to-leading order. Such high orders will not be considered explicitly below.

3 Pionless Theory

Before we discuss the TV potential in ChPT, it is instructive to consider a much simpler EFT. At momenta much smaller than the pion mass, pion degrees of freedom can be integrated out and one is left with a pionless EFT, in which the interactions are represented by operators involving only nucleon fields. If we denote by $M_{\text{nuc}} \sim 100$ MeV the scales associated with pion physics, this EFT applies to processes where all momenta $Q \ll M_{\text{nuc}}$. Power counting in this EFT is different from ChPT and is reviewed in Ref. [48].

The lowest-order TC two-nucleon interactions can be taken as [66]

$$\mathcal{L}_{\vec{\tau},T}^{(0)} = -\frac{C_{11}}{2} \bar{N} N \bar{N} N - \frac{C_{\tau\tau}}{2} \bar{N} \vec{\tau} N \cdot \bar{N} \vec{\tau} N, \quad (43)$$

where $C_{11,\tau\tau} = \mathcal{O}(4\pi/m_N \mathfrak{N})$, with $\mathfrak{N} < M_{\text{nuc}}$ a low-energy scale. The corresponding potential in momentum space is simply

$$V_{\vec{\tau},T}^{(0)} = \frac{1}{2} \left[C_{11} + C_{\tau\tau} \vec{\tau}^{(1)} \cdot \vec{\tau}^{(2)} \right], \quad (44)$$

where $\vec{\tau}^{(i)}/2$ is the isospin of nucleon i . These interactions affect only the two S waves. Since the effect of free two-nucleon propagation is $\sim m_N Q / 4\pi$, for momenta $Q \gtrsim \mathfrak{N}$ these interactions have to be iterated to all orders [78, 79]. Using dimensional regularization with power divergence subtraction [79] at a scale μ ,

$$C_{0s} = C_{11} - 3C_{\tau\tau} = \frac{4\pi}{m_N} \left(\frac{1}{a_s} - \mu \right)^{-1}, \quad C_{0t} = C_{11} + C_{\tau\tau} = \frac{4\pi}{m_N} \left(\frac{1}{a_t} - \mu \right)^{-1}, \quad (45)$$

in terms of the isospin-singlet (3S_1) and -triplet (1S_0) scattering lengths, a_s and a_t . Because the coefficients $C_{11,\tau\tau}$ subsume physics at the scale of the pion mass, their scaling is different from the one in the pionful EFT.

In leading order, the $\bar{\theta}$ term and the dimension-6 sources induce TV four-nucleon operators similar to those in Eqs. (27), (41) and (42):

$$\begin{aligned}\mathcal{L}_{\not{T},T} = & \bar{C}_{11}\bar{N}N\partial_\mu(\bar{N}S^\mu N) + \bar{C}_{\tau\tau}\bar{N}\vec{\tau}N\cdot\partial_\mu(\bar{N}S^\mu\vec{\tau}N) \\ & + \bar{C}_{31}\bar{N}\tau_3N\partial_\mu(\bar{N}S^\mu N) + \bar{C}_{13}\bar{N}N\cdot\partial_\mu(\bar{N}S^\mu\tau_3N) + \bar{C}_{33}\bar{N}\tau_3N\partial_\mu(\bar{N}S^\mu\tau_3N),\end{aligned}\quad (46)$$

where $\bar{C}_{11,\tau\tau,13,31,33}$ are new short-range parameters. In momentum space the interaction Hamiltonian is given by

$$\begin{aligned}V_{\not{T},T}(\vec{q}) = & -\frac{i}{2}\left[\bar{C}_{11} + \bar{C}_{\tau\tau}\vec{\tau}^{(1)}\cdot\vec{\tau}^{(2)} + \bar{C}_{33}\tau_3^{(1)}\tau_3^{(2)}\right]\left(\vec{\sigma}^{(1)} - \vec{\sigma}^{(2)}\right)\cdot\vec{q} \\ & -\frac{i}{4}\left(\bar{C}_{13} + \bar{C}_{31}\right)\left(\tau_3^{(1)} + \tau_3^{(2)}\right)\left(\vec{\sigma}^{(1)} - \vec{\sigma}^{(2)}\right)\cdot\vec{q} \\ & -\frac{i}{4}\left(\bar{C}_{13} - \bar{C}_{31}\right)\left(\tau_3^{(1)} - \tau_3^{(2)}\right)\left(\vec{\sigma}^{(1)} + \vec{\sigma}^{(2)}\right)\cdot\vec{q},\end{aligned}\quad (47)$$

where $\vec{\sigma}^{(i)}/2$ is the spin of nucleon i and $\vec{q} = \vec{p}_1 - \vec{p}_1' = \vec{p}_2' - \vec{p}_2$ is the momentum transfer.

In nucleon-nucleon scattering, operators that break P and T induce mixing between waves of different parity. At low energy, the most relevant effect is the mixing between S and P waves, and indeed the single momentum in Eq. (47) can only connect an S to a P wave. At leading order, the P wave is free. Since the short-range TV potential involves one S wave, we expect [48] that in the pionless EFT the coefficients \bar{C}_{ij} scale as $1/\aleph$. Indeed, the amplitude for a nucleon-nucleon transition can be computed from Eq. (47) as done in the PV case in Refs. [56, 60]. In leading order, it involves one insertion of the TV operators \bar{C}_{ij} , dressed by the all-order iteration of the appropriate S -wave operator, C_{0s} or C_{0t} . The renormalization-group invariance of the amplitude implies that the \bar{C}_{ij} follow a renormalization-group equation of the form $d(\bar{C}_{ij}/C_0)/d\ln\mu = 0$, which is satisfied if the five independent parameters are taken to be

$$\begin{aligned}\bar{C}_{1s} = \bar{C}_{11} - 3\bar{C}_{\tau\tau} &= \frac{4\pi\bar{c}_s}{m_N}\left(\frac{1}{a_s} - \mu\right)^{-1}, \quad \bar{C}_{1t} = \bar{C}_{11} + \bar{C}_{\tau\tau} = \frac{4\pi\bar{c}_t}{m_N}\left(\frac{1}{a_t} - \mu\right)^{-1}, \\ \bar{C}_{3s} = \bar{C}_{13} - \bar{C}_{31} &= \frac{4\pi\bar{c}_{3s}}{m_N}\left(\frac{1}{a_s} - \mu\right)^{-1}, \quad \bar{C}_{3t} = \bar{C}_{13} + \bar{C}_{31} = \frac{4\pi\bar{c}_{3t}}{m_N}\left(\frac{1}{a_t} - \mu\right)^{-1}, \\ \bar{C}_{33} &= \frac{4\pi\bar{c}_{33t}}{m_N}\left(\frac{1}{a_t} - \mu\right)^{-1},\end{aligned}\quad (48)$$

in terms of five μ -independent coefficients $\bar{c}_{s,t,3s,3t,33t}$. As in the TC sector, the scaling of the short-range parameters is different in the pionless EFT than in ChPT. We can write

$$\bar{C}_{11,\tau\tau} = \mathcal{O}\left(\frac{4\pi}{m_N\aleph}\bar{c}_{s,t}\right), \quad \bar{C}_{13,31} = \mathcal{O}\left(\frac{4\pi}{m_N\aleph}\bar{c}_{3s,3t}\right), \quad \bar{C}_{33} = \mathcal{O}\left(\frac{4\pi}{m_N\aleph}\bar{c}_{33t}\right). \quad (49)$$

In order to estimate the coefficients $\bar{c}_{s,t,3s,3t,33t}$, we use naive dimensional analysis [17, 65, 9] with the pionful EFT as the underlying theory. We then find that at leading order the isoscalar $\bar{c}_{s,t}$ receive contributions from all the sources,

$$\bar{c}_{s,t} = \mathcal{O}\left(\frac{\bar{\theta}}{M_{QCD}}, (\tilde{\delta}_0 + \varepsilon\tilde{\delta}_3)\frac{M_{QCD}}{M_F^2}, \frac{\alpha_{\text{em}}}{4\pi}(\delta_0 + \delta_3)\frac{M_{QCD}}{M_F^2}, w\frac{M_{QCD}}{M_F^2}\right), \quad (50)$$

while the isospin-breaking $\bar{c}_{3s,3t}$ only from the dimension-6 sources,

$$\bar{c}_{3s,3t} = \mathcal{O}\left(\tilde{\delta}_3\frac{M_{QCD}}{M_F^2}, \frac{\alpha_{\text{em}}}{4\pi}(\delta_0 + \delta_3)\frac{M_{QCD}}{M_F^2}, \varepsilon w\frac{M_{QCD}}{M_F^2}\right), \quad (51)$$

and \bar{c}_{33t} only from the qEDM,

$$\bar{c}_{33t} = \mathcal{O} \left(\frac{\alpha_{\text{em}}}{4\pi} \delta_3 \frac{M_{QCD}}{M_T^2} \right). \quad (52)$$

In general, one would expect five possible amplitudes connecting S to P waves [34, 46]: three—one for each possible value of $I_3 = 1, 0, -1$ —to describe the mixing of the isotriplet 1S_0 and 3P_0 waves, one for the mixing of the isosinglet 3S_1 and 1P_1 states, and one for the mixing of nucleons in the 3S_1 configuration with the isotriplet 3P_1 wave. The $\bar{\theta}$ term yields a short-range potential in the form of the isospin-conserving terms of Ref. [34]. Because the TV operator in Eq. (21) is isoscalar and isospin violation is a subleading effect in ChPT, for which the pionless EFT is the low-energy limit, the $\bar{\theta}$ term does not contribute at leading order to quantities that violate both T and isospin. The two terms contribute to 3S_1 – 1P_1 mixing and to 1S_0 – 3P_0 mixing, in equal way for the three I_3 configurations. The 3S_1 – 3P_1 mixing vanishes at leading order, a fact that has important consequences for the estimate of the deuteron EDM [28]. If $\tilde{\delta}_3$ and ε are different from zero, the qCEDM and the chiral-invariant TV sources also contribute to isospin-breaking TV observables at leading order. The operator \bar{C}_{3t} is proportional to the third component of the total isospin of the two-nucleon pair, and thus it does contribute to 1S_0 – 3P_0 mixing, but only for $I_3 = \pm 1$. \bar{C}_{3s} is instead proportional to the total spin of the two nucleons, and it is relevant to 3S_1 – 3P_1 mixing, and, consequently, to the deuteron EDM. Only the qEDM produces full isospin breaking in leading order.

A potential with just these five short-range terms was considered recently [47]. Five low-energy quantities—such as the spin rotation of a polarized beam and the longitudinal polarization of an unpolarized incident beam in neutron scattering on a proton target [46] at different energies—are needed to determine the parameters $\bar{c}_{s,t}$, $\bar{c}_{3s,3t}$, and \bar{c}_{33t} .

There is, however, an important extra ingredient that needs to be added at low energies: one-photon exchange where one of the vertices originates in the nucleon EDM, as in Eq. (40), see Fig. 1. This long-range potential is particularly important for qEDM, since for this source the short-range interactions have suppression by $\alpha_{\text{em}}/4\pi$ from the hard photon, as can be seen in Eqs. (50), (51), and (52). We find

$$\begin{aligned} V_{\gamma,T}(\vec{q}) = & -\frac{ie}{2} \left[\bar{d}_0 + \bar{d}_1 \tau_3^{(1)} \tau_3^{(2)} \right] \left(\vec{\sigma}^{(1)} - \vec{\sigma}^{(2)} \right) \cdot \frac{\vec{q}}{q^2} \\ & -\frac{ie}{4} \left[(\bar{d}_0 + \bar{d}_1) \left(\tau_3^{(1)} + \tau_3^{(2)} \right) \left(\vec{\sigma}^{(1)} - \vec{\sigma}^{(2)} \right) + (\bar{d}_1 - \bar{d}_0) \left(\tau_3^{(1)} - \tau_3^{(2)} \right) \left(\vec{\sigma}^{(1)} + \vec{\sigma}^{(2)} \right) \right] \cdot \frac{\vec{q}}{q^2}, \end{aligned} \quad (53)$$

where

$$\bar{d}_{0,1} = \mathcal{O} \left(e \delta_{0,3} \frac{m_\pi^2}{M_T^2 M_{QCD}} \right) \quad (54)$$

are the isoscalar and isovector components of the nucleon EDM. In principle, the coefficients $\bar{d}_{0,1}$ in the pionless theory are different from the short-range contributions to the nucleon EDM in the pionful theory introduced in Eq. (40). However, since in the case of TV from the qEDM pion-loop contributions to the nucleon EDM are suppressed [24], at leading order they exactly match.

The photon-exchange potential has the same spin/isospin components of the short-range potential (47), but it acts on all partial waves. While for the other sources this type of potential is important only for very low momenta, for qEDM it is enhanced with respect to the short-range potential (47) by a factor of M_{nuc}/\aleph for $Q \sim \aleph$, and it dominates throughout the regime of the pionless EFT.

In subleading orders more derivatives appear in two-nucleon contact interactions and photon exchange. An important issue is the order where few-nucleon forces first appear. On the basis of naive dimensional analysis, we expect them to be also of subleading order. In the PV TC case, this is confirmed for the three-nucleon force by a more detailed analysis based on renormalization-group invariance [58]. Since the powers of momenta involved here are the same, the same conclusion should hold. The potentials (47) and (53) should then be sufficient for most TV applications of the pionless EFT.

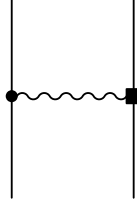


Figure 1: One-photon-exchange diagram contributing to the long-range TV two-nucleon potential. The solid and wavy lines represent nucleon and photon, respectively; a square stands for the TV photon-nucleon couplings in $\mathcal{L}_{f=2,T6}^{(1)}$ (40), while the filled circle represents an interaction from $\mathcal{L}_{f\leq 2,T}^{(0)}$ (15). Only one possible ordering is shown.

4 The TV Potential in Momentum Space

In processes involving momenta $Q \sim M_{nuc}$, which presumably comprise the bound states of most nuclei, pion effects are important and pion degrees of freedom should be included explicitly in the theory. In this section we use the interactions given in Sect. 2 to compute the TV nuclear potential in momentum space for the TV sources of dimension up to 6.

In the lowest orders, the TV nuclear potential involves only two nucleons. We write the two incoming momenta as $\vec{p}_1 = \vec{P}/2 + \vec{p}$ and $\vec{p}_2 = \vec{P}/2 - \vec{p}$, and the two outgoing momenta as $\vec{p}'_1 = \vec{P}/2 + \vec{p}'$ and $\vec{p}'_2 = \vec{P}/2 - \vec{p}'$. The TV potential in momentum space can be expressed as function not only of the momentum transfer $\vec{q} = \vec{p} - \vec{p}'$, but also of the center-of-mass (CM) momentum \vec{P} and of the variable $\vec{K} = (\vec{p} + \vec{p}')/2$: $V_T = V_T(\vec{q}, \vec{K}, \vec{P})$. Expressions for the potential in the CM frame are obtained by setting $\vec{P} = 0$. Notice that although some of the terms below vanish in the CM frame, they can be relevant to the calculation of the TV electromagnetic form factors of deuteron, or for calculations of T violation in nuclei with $A > 2$, where the interaction with the photon or other nucleons changes the CM momentum of the nucleon pair.

4.1 $\bar{\theta}$ Term

In leading order, the $\bar{\theta}$ -term nuclear potential comes from the OPE diagrams of Fig. 2, with TC and TV pion-nucleon interactions taken from $\mathcal{L}_{f\leq 2,T}^{(0)}$ and $\mathcal{L}_{f=2,T4}^{(1)}$ in Eqs. (15) and (22), respectively. The strong-interaction vertex introduces a factor of $g_A Q/F_\pi$, while the TV vertex brings in a factor $\bar{g}_0 \propto m_\pi^2/M_{QCD}$. As a result this contribution goes as M_{QCD}^{-1} and it is of order $\nu = 1$. In momentum space, the expression for the potential is simply

$$V_{\bar{\theta}}^{(1)} = i \frac{g_A \bar{g}_0}{F_\pi^2} \vec{\tau}^{(1)} \cdot \vec{\tau}^{(2)} \left(\vec{\sigma}^{(1)} - \vec{\sigma}^{(2)} \right) \cdot \frac{\vec{q}}{\vec{q}^2 + m_\pi^2}, \quad (55)$$

which agrees with Ref. [29]. Just like the $\bar{\theta}$ term contribution to the potential (47) in the pionless theory, this OPE potential contributes to 1S_0 - 3P_0 and 3S_1 - 1P_1 mixing, but not to the isospin-violating 3S_1 - 3P_1 mixing. At this order, there is a single unknown TV parameter, \bar{g}_0 . Contrary to the PC, TC case [48] and more like the PV, TC potential [56], pion physics is enhanced relative to short-range physics due to the absence of a derivative in the simplest pion-nucleon TV interaction and the presence of one in the simplest TV two-nucleon contact interaction.

Since in nuclei the OPE from the $I = 0$ pion-nucleon coupling \bar{g}_0 is suppressed by the factor $(N - Z)/A$, it is interesting to pursue higher orders, up until the $I = 1$ pion-nucleon coupling \bar{g}_1 , whose OPE is not affected by such suppression, appears. This means up to $\nu = 3$, that is, including corrections of $\mathcal{O}(Q^2/M_{QCD}^2)$ with respect to the leading TV potential. According to Eq. (13), corrections at orders $\nu = 2, 3$ come from one-loop diagrams involving $\mathcal{L}_{f\leq 2,T}^{(0)}$ and $\mathcal{L}_{f=2,T4}^{(1)}$ only, and from tree diagrams with

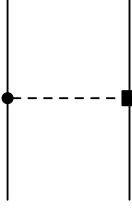


Figure 2: OPE diagram contributing to the leading TV two-nucleon potential. The solid and dashed lines represent nucleon and pion, respectively; a square stands for the TV pion-nucleon couplings \bar{g}_0 in $\mathcal{L}_{f=2,T4}^{(1)}$ (22) or $\bar{g}_{0,1,2}$ and \bar{t}_1 in $\mathcal{L}_{f=2,T6}^{(\Delta_\pi)}$ (39), while the filled circle represents an interaction from $\mathcal{L}_{f\leq 2,T}^{(0)}$ (15). Only one possible ordering is shown.

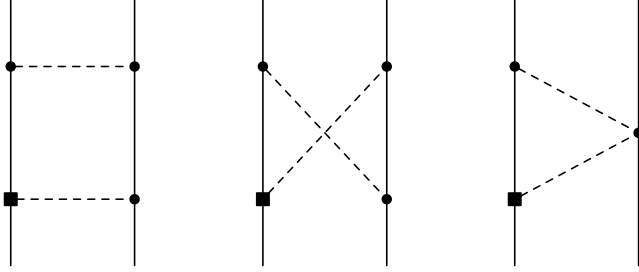


Figure 3: Box, crossed, and triangle TPE diagrams contributing to the subleading TV two-nucleon potential. Notation as in Fig. 2. Only one possible ordering per topology is shown.

insertions of higher-order terms. The tree contributions come from the four-nucleon TV operators in $\mathcal{L}_{f=4,T4}^{(3)}$, Eq. (27), and from OPE diagrams in which either the TC or the TV vertices originate in the power-suppressed $f \leq 2$ Lagrangians.

The most important loop diagrams are from TPE, depicted in Fig. 3. The T -odd pion-nucleon coupling \bar{g}_0 and one of the strong-interaction vertices bring in a factor of $\bar{g}_0 g_A / F_\pi^2$. The other two vertices of the box and crossed diagrams of Fig. 3 are strong-interaction pion-nucleon vertices from Eq. (15), and combined with the $(4\pi)^2$ from the loop integration, they yield the suppression factor $g_A^2 / (4\pi F_\pi)^2 \sim 1/M_{QCD}^2$. For the triangle diagrams, the seagull vertex is the Weinberg-Tomozawa term also from Eq. (15), which brings in a factor of $1/F_\pi^2$ that, combined with the $(4\pi)^2$ from the loop, also leads to a suppression of $1/(4\pi F_\pi)^2 \sim 1/M_{QCD}^2$. All these diagrams are thus of order M_{QCD}^{-3} . Care of course has to be taken with the subtraction from the box diagrams in Fig. 3 of the iterated static OPE, which is infrared enhanced and already included in the computation of wave functions at lower order. Following the procedure described for instance in Ref. [56], the subtraction is accomplished by exploiting the identity

$$\frac{i}{-v \cdot k + i\varepsilon} = -\frac{i}{v \cdot k + i\varepsilon} + 2\pi\delta(v \cdot k). \quad (56)$$

When Eq. (56) is used in place of one of the nucleon propagators in the box diagrams, the first term on the right-hand side leads to a contour integral over the 0th component of the loop momentum, which can be performed without picking up the nucleon poles and is free of the infrared enhancement discussed in Sect. 2, while the delta function corresponds to the two-nucleon pole and must be discarded in the calculation of the potential. For the crossed-box and triangle diagrams, instead, it is always possible to avoid the nucleon poles, and these diagrams only contribute to the potential.

The TPE diagrams in Fig. 3 are ultraviolet divergent. We regulate them in dimensional regularization

in d spacetime dimensions, where divergences get encoded in the factor

$$L = \frac{2}{4-d} - \gamma_E + \ln 4\pi, \quad (57)$$

where γ_E is the Euler constant. We denote by μ the renormalization scale. Proper renormalization requires that sufficiently many counterterms appear at the same order to compensate for the L and μ dependence of the loops. Indeed, here this dependence can be absorbed by the renormalization of the contact interaction \bar{C}_2 from $\mathcal{L}_{f=4,T^4}^{(3)}$, Eq. (27), which we do by redefining it through

$$\bar{C}_2 \rightarrow \bar{C}_2 + \frac{2g_A\bar{g}_0}{F_\pi^2} \frac{1}{(2\pi F_\pi)^2} \left[(3g_A^2 - 1) \left(L + \ln \frac{\mu^2}{m_\pi^2} \right) + 2(g_A^2 - 1) \right]. \quad (58)$$

Note that we chose to absorb in \bar{C}_2 some finite constant pieces. TPE does not renormalize the coupling \bar{C}_1 at this order. With this redefinition, the contact interactions yield the short-range potential

$$V_{\bar{\theta},\text{SR}}^{(3)}(\vec{q}) = -\frac{i}{2} \left[\bar{C}_1 + \bar{C}_2 \vec{\tau}^{(1)} \cdot \vec{\tau}^{(2)} \right] \left(\vec{\sigma}^{(1)} - \vec{\sigma}^{(2)} \right) \cdot \vec{q}, \quad (59)$$

which is formally identical to the leading $\bar{\theta}$ potential in the pionless EFT, Eq. (47). The couplings, however, are different. We can see from Eq. (58) that the natural size of the coefficients \bar{C}_i is, as advertised, $\bar{\theta}m_\pi^2/F_\pi^2 M_{QCD}^3$, implying a suppression of Q^2/M_{QCD}^2 with respect to TV OPE.

Once the divergent, short-range part of TPE has been lumped with the contact terms, we are left with the non-analytic contributions of medium range,

$$V_{\bar{\theta},\text{MR}}^{(3)} = -i \frac{2\bar{g}_0 g_A}{F_\pi^2} \frac{1}{(2\pi F_\pi)^2} \left[2g_A^2 B \left(\frac{\vec{q}^2}{4m_\pi^2} \right) - T \left(\frac{\vec{q}^2}{4m_\pi^2} \right) \right] \vec{\tau}^{(1)} \cdot \vec{\tau}^{(2)} \left(\vec{\sigma}^{(1)} - \vec{\sigma}^{(2)} \right) \cdot \vec{q}, \quad (60)$$

in terms of the functions

$$T(x) = \sqrt{\frac{1+x}{x}} \ln(\sqrt{x} + \sqrt{1+x}) = \frac{1+x}{1+\frac{3}{2}x} B(x). \quad (61)$$

As the leading OPE potential, Eq. (55), the TPE potential is a function only of the momentum transfer \vec{q} . The scale of momentum variation is, as one would expect, $2m_\pi$. TPE and leading OPE share the same spin-isospin structure, which means they can only be separated if we probe their different momentum dependences.

A much richer structure arises from the remaining $\nu \leq 3$ contributions to the two-nucleon TV potential, which come from the OPE diagrams depicted in Fig. 4. Doubly-circled vertices in the first two diagrams denote $\mathcal{O}(Q^2/M_{QCD}^2)$ corrections to the TC and TV pion-nucleon couplings, given by the operators in the Lagrangians $\mathcal{L}_{f \leq 2, TI}^{(1,2)}$, $\mathcal{L}_{f \leq 2, TI}^{(1,2)}$, and $\mathcal{L}_{f=2, T^4}^{(3)}$ found in Eqs. (16), (17), (20), and (24). The last diagram is proportional to corrections to the pion mass in $\mathcal{L}_{f \leq 2, TI}^{(2)}$ and $\mathcal{L}_{f \leq 2, TI}^{(1,2)}$, and to the nucleon mass difference in $\mathcal{L}_{f \leq 2, TI}^{(1,2)}$. Note that, as we argue shortly, there are no further loop diagrams to consider explicitly.

Corrections that originate in the pion mass are closely connected to the leading OPE, Eq. (55). At the order we are considering, the pion mass receives corrections from one-loop diagrams, which we absorb [18] in the renormalization of the coupling Δm_π^2 in Eq. (17). With the definitions of Eqs. (15), (17), (18), and (19), the physical masses of the neutral and charged pions are, respectively, $m_{\pi^0}^2 = m_\pi^2 + \Delta m_\pi^2 + \delta m_\pi^2 = (135 \text{ MeV})^2$ and $m_{\pi^\pm}^2 = m_\pi^2 + \Delta m_\pi^2 + \check{\delta} m_\pi^2 = (139.6 \text{ MeV})^2$ [72]. The isospin-symmetric correction to the pion mass can be accounted at $\nu = 3$ by substituting $m_\pi^2 \rightarrow m_\pi^2 + \Delta m_\pi^2$ in the leading-order TV potential. Isospin-breaking corrections come from the different masses of the neutral and charged pions. With the assumption $\alpha_{\text{em}}/4\pi \sim \varepsilon m_\pi^3/M_{QCD}^3$, which is numerically reasonable, the pion mass splitting is dominated by the electromagnetic contribution $\check{\delta} m_\pi^2$, which gives rise to a potential of order $\nu = 2$. The

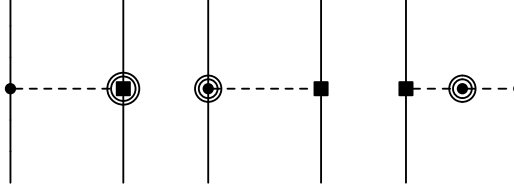


Figure 4: OPE corrections to the $\bar{\theta}$ -term two-nucleon potential up to order $\mathcal{O}(Q^3/M_{QCD}^3)$. The double circles denote vertices in the $\Delta = 1, 2$ TC chiral Lagrangians, $\mathcal{L}_{f \leq 2, TI}^{(1)}$ (16), $\mathcal{L}_{f \leq 2, TI}^{(2)}$ (17), and $\mathcal{L}_{f \leq 2, TI}^{(1,2)}$ (20). The doubly-circled square denotes vertices from the $\Delta = 3$ TV Lagrangian, $\mathcal{L}_{f=2, T4}^{(3)}$ (24). Other notation as in Fig. 2. Only one possible ordering is shown.

quark-mass-difference contribution δm_π^2 appears at $\nu = 3$, when one should also consider diagrams with two insertions of $\check{\delta} m_\pi^2$. The sum of these components generates two structures, an isoscalar

$$V_{\bar{\theta},a}^{(2+3)}(\vec{q}) = -i \frac{\bar{g}_0 g_A}{3F_\pi^2} \left(2\check{\delta} m_\pi^2 + \delta m_\pi^2 - 2 \frac{(\check{\delta} m_\pi^2)^2}{q^2 + m_\pi^2} \right) \vec{\tau}^{(1)} \cdot \vec{\tau}^{(2)} \left(\vec{\sigma}^{(1)} - \vec{\sigma}^{(2)} \right) \cdot \frac{\vec{q}}{(\vec{q}^2 + m_\pi^2)^2}, \quad (62)$$

and an isotensor

$$V_{\bar{\theta},b}^{(2+3)}(\vec{q}) = i \frac{\bar{g}_0 g_A}{3F_\pi^2} \left(\check{\delta} m_\pi^2 - \delta m_\pi^2 - \frac{(\check{\delta} m_\pi^2)^2}{q^2 + m_\pi^2} \right) \left(3\tau_3^{(1)} \tau_3^{(2)} - \vec{\tau}^{(1)} \cdot \vec{\tau}^{(2)} \right) \left(\vec{\sigma}^{(1)} - \vec{\sigma}^{(2)} \right) \cdot \frac{\vec{q}}{(\vec{q}^2 + m_\pi^2)^2}. \quad (63)$$

These isoscalar and isotensor components can be rewritten using the physical pion masses. The isoscalar component, Eq. (62), can be obtained by using the physical values of the neutral and charged pion mass in the leading potential, Eq. (55). We can write

$$V_{\bar{\theta}}^{(1)}(\vec{q}) + V_{\bar{\theta},a}^{(2+3)}(\vec{q}) = i \frac{\bar{g}_0 g_A}{3F_\pi^2} \left(\frac{2}{\vec{q}^2 + m_{\pi^\pm}^2} + \frac{1}{\vec{q}^2 + m_{\pi^0}^2} \right) \vec{\tau}^{(1)} \cdot \vec{\tau}^{(2)} \left(\vec{\sigma}^{(1)} - \vec{\sigma}^{(2)} \right) \cdot \vec{q}, \quad (64)$$

which, expanding in $\check{\delta} m_\pi^2$ and δm_π^2 , reproduces Eq. (62). The combination of neutral and charged pion propagators in Eq. (64) represents an “average” pion static propagator, which naturally appears in the isoscalar contribution. Similarly, we can rewrite the tensor component as

$$V_{\bar{\theta},b}^{(2+3)}(\vec{q}) = -i \frac{\bar{g}_0 g_A}{3F_\pi^2} \left(\frac{1}{\vec{q}^2 + m_{\pi^\pm}^2} - \frac{1}{\vec{q}^2 + m_{\pi^0}^2} \right) \left(3\tau_3^{(1)} \tau_3^{(2)} - \vec{\tau}^{(1)} \cdot \vec{\tau}^{(2)} \right) \left(\vec{\sigma}^{(1)} - \vec{\sigma}^{(2)} \right) \cdot \vec{q}. \quad (65)$$

In applications to nucleon-nucleon scattering, this tensor component would contribute at low energies to 1S_0 - 3P_0 mixing, affecting proton-proton and neutron-neutron ($I_3 = \pm 1$) and neutron-proton ($I_3 = 0$) scattering differently. It is worth stressing that, in contrast to phenomenological approaches, the isotensor component coming from the $\bar{\theta}$ term is not a leading contribution.

Corrections from the nucleon mass come in several guises. The use of a heavy-nucleon field ensures that the large scale m_N appears always in denominators. In the isospin-symmetric limit the first effects of m_N enter in the $\Delta = 1, 2$ TC Lagrangians, Eqs. (16) and (17), the $\Delta = 3$ TV Lagrangian, Eq. (24), and, via the on-shell condition for the nucleons, the energy of the potential-pion propagator. They yield relativistic corrections to the leading OPE with the same spin-isospin structure,

$$V_{\bar{\theta},c}^{(3)}(\vec{q}, \vec{K}, \vec{P}) = -i \frac{g_A \bar{g}_0}{F_\pi^2 m_N^2} \left(\vec{K}^2 + \frac{\vec{P}^2}{4} - \frac{1}{4} \frac{(\vec{P} \cdot \vec{q})^2}{\vec{q}^2 + m_\pi^2} \right) \vec{\tau}^{(1)} \cdot \vec{\tau}^{(2)} \left(\vec{\sigma}^{(1)} - \vec{\sigma}^{(2)} \right) \cdot \frac{\vec{q}}{\vec{q}^2 + m_\pi^2}, \quad (66)$$

and with new structures,

$$\begin{aligned}
V_{\theta,d}^{(3)}(\vec{q}, \vec{K}, \vec{P}) = & -i \frac{g_A \bar{g}_0}{4F_\pi^2 m_N^2} \vec{\tau}^{(1)} \cdot \vec{\tau}^{(2)} \frac{1}{\vec{q}^2 + m_\pi^2} \left\{ \vec{P} \cdot \vec{q} \left[\left(\vec{\sigma}^{(1)} - \vec{\sigma}^{(2)} \right) \cdot \frac{\vec{P}}{2} + \left(\vec{\sigma}^{(1)} + \vec{\sigma}^{(2)} \right) \cdot \vec{K} \right] \right. \\
& \left. + i \vec{\sigma}^{(1)} \cdot \left[\vec{q} \times \left(\frac{\vec{P}}{2} + \vec{K} \right) \right] \vec{\sigma}^{(2)} \cdot \vec{q} + i \vec{\sigma}^{(1)} \cdot \vec{q} \vec{\sigma}^{(2)} \cdot \left[\vec{q} \times \left(\frac{\vec{P}}{2} - \vec{K} \right) \right] \right\}. \quad (67)
\end{aligned}$$

Note that in writing Eqs. (66) and (67) we have omitted pieces that vanish due to energy-momentum conservation for on-shell nucleons, which implies $\vec{K} \cdot \vec{q} = \vec{p}^2 - \vec{p}'^2 = 0$. This potential includes the contribution of the $1/m_N$ correction to g_A in Eq. (16). Naively, one would expect this correction to contribute at order $\nu = 2$; however the interaction brings in a factor of $v \cdot q$, which, for on-shell nucleons, becomes $v \cdot q = \vec{q} \cdot \vec{P}/2m_N$, suppressing the potential by a further factor of $1/m_N$. There is a subtlety in this argument. When one performs the integral involving both OPE with a pion energy in the numerator and another interaction in the potential, and picks the pion pole, one gets a one-loop contribution to the potential. However, by power counting, such diagrams are suppressed by a further Q/M_{QCD} . (This of course does not preclude enhancements by factors of π that in principle might affect any ChPT loop, but are hard to incorporate in power counting.)

Corrections to the nucleon mass can be removed from nucleon propagators by redefinitions of the nucleon field. The chiral-symmetry-breaking correction to the nucleon mass, Δm_N in Eq. (16), can be absorbed in m_N , $m_N \rightarrow m_N - \Delta m_N$, by a redefinition of the nucleon field of the same type of that which eliminates the mass from Eq. (15) in the first place. The isospin-violating nucleon mass splittings δm_N and $\check{\delta} m_N$ can be dealt with the field redefinition of Ref. [54], which leads to Eq. (20). The corresponding potential linear in δm_N has a $1/m_N$ factor,

$$\begin{aligned}
V_{\theta,e}^{(3)}(\vec{q}, \vec{K}, \vec{P}) = & \frac{\bar{g}_0 g_A}{F_\pi^2} \frac{\delta m_N}{m_N} \frac{1}{\vec{q}^2 + m_\pi^2} \left(\vec{\tau}^{(1)} \times \vec{\tau}^{(2)} \right)_3 \\
& \left[\left(\vec{\sigma}^{(1)} + \vec{\sigma}^{(2)} \right) \cdot \vec{K} + \left(\vec{\sigma}^{(1)} - \vec{\sigma}^{(2)} \right) \cdot \left(\frac{\vec{P}}{2} + \frac{\vec{q}}{\vec{q}^2 + m_\pi^2} \vec{P} \cdot \vec{q} \right) \right]. \quad (68)
\end{aligned}$$

This potential has the right quantum numbers to produce 3S_1 - 3P_1 mixing, and therefore must be included in a calculation of the deuteron EDM. In addition, there are terms quadratic in δm_N , which generate an additional contribution to the isoscalar and tensor potentials in Eqs. (62) and (63),

$$V_{\theta,f}^{(3)}(\vec{q}) = i \frac{\bar{g}_0 g_A}{3F_\pi^2} \delta m_N^2 \left[2\vec{\tau}^{(1)} \cdot \vec{\tau}^{(2)} - \left(3\tau_3^{(1)} \tau_3^{(2)} - \vec{\tau}^{(1)} \cdot \vec{\tau}^{(2)} \right) \right] \left(\vec{\sigma}^{(1)} - \vec{\sigma}^{(2)} \right) \cdot \frac{\vec{q}}{(\vec{q}^2 + m_\pi^2)^2}. \quad (69)$$

Note that the electromagnetic correction to the nucleon mass, $\check{\delta} m_N$, does not appear in the equations above. The reason is that in Eq. (20) it appears with a $v \cdot \partial \vec{\pi}$ factor, which again brings a $v \cdot q$ and consequently an extra suppression $\sim Q/m_N$. The contribution from $\check{\delta} m_N$ is thus next order. Up to such higher-order terms, we can make $\delta m_N \rightarrow \delta m_N + \check{\delta} m_N = m_n - m_p$ in the expressions above.

Finally we arrive at contributions from $\nu = 3$ effects in the pion-nucleon vertices. At this order, several contributions can be absorbed into redefinitions of the couplings g_A , \bar{g}_0 , and \bar{C}_2 . One-loop corrections to g_A do not introduce any non-analytic contribution and, for an on-shell nucleon, they renormalize the coupling d_A in Eq. (17) [80]. The operator with coefficient d_A gives rise to a potential like Eq. (55), with g_A replaced by $-g_A d_A$. For simplicity we absorb d_A in g_A , $g_A \rightarrow g_A(1 + d_A)$. Similarly, the calculation of the pion-nucleon TV form factor in Ref. [25] shows that the one-loop corrections to \bar{g}_0 do not introduce any non-trivial momentum dependence, so they simply renormalize the coupling $\Delta \bar{g}_0$ in Eq. (24). These m_π^2 corrections to \bar{g}_0 can be absorbed in it, $\bar{g}_0 \rightarrow \bar{g}_0 - \Delta \bar{g}_0 + \bar{g}_0 \delta m_\pi^2 / m_\pi^2$. As for the operators with coefficients c_A in Eq. (17) and $\bar{\eta}$ in Eq. (24), they give potentials of the form

$$\vec{\tau}^{(1)} \cdot \vec{\tau}^{(2)} \left(\vec{\sigma}^{(1)} - \vec{\sigma}^{(2)} \right) \cdot \vec{q} \frac{\vec{q}^2}{\vec{q}^2 + m_\pi^2} = -\vec{\tau}^{(1)} \cdot \vec{\tau}^{(2)} \left(\vec{\sigma}^{(1)} - \vec{\sigma}^{(2)} \right) \cdot \vec{q} \frac{m_\pi^2}{\vec{q}^2 + m_\pi^2} + \vec{\tau}^{(1)} \cdot \vec{\tau}^{(2)} \left(\vec{\sigma}^{(1)} - \vec{\sigma}^{(1)} \right) \cdot \vec{q}, \quad (70)$$

which cannot be distinguished from those of $g_A\bar{g}_0$ and \bar{C}_2 , and can therefore be absorbed into further redefinitions of g_A , \bar{g}_0 , and \bar{C}_2 . Now the Goldberger-Treiman relation for the strong pion-nucleon constant, $g_{\pi NN} = 2m_N g_A / F_\pi$, applies without an explicit correction. If for the pion-nucleon coupling constant we use $g_{\pi NN} = 13.07$ [81], then in the leading-order TV potential we should use $g_A = 1.29$.

The remaining contributions come from vertex corrections, both in the TV sector via the TV pion-nucleon coupling $\pi_3 \bar{N}N$ in Eq. (24), and in the TC sector via the isospin-breaking pion-nucleon axial-vector coupling $\partial_\mu \pi_3 \bar{N} S^\mu N$ in Eq. (20). We find

$$V_{\bar{\theta},g}^{(3)}(\vec{q}) = \frac{i}{2F_\pi^2} \frac{1}{\vec{q}^2 + m_\pi^2} \left\{ \left(g_A \bar{g}_1 - \frac{\bar{g}_0 \beta_1}{2} \right) \left(\tau_3^{(1)} + \tau_3^{(2)} \right) \left(\vec{\sigma}^{(1)} - \vec{\sigma}^{(2)} \right) \cdot \vec{q} \right. \\ \left. + \left(g_A \bar{g}_1 + \frac{\bar{g}_0 \beta_1}{2} \right) \left(\tau_3^{(1)} - \tau_3^{(2)} \right) \left(\vec{\sigma}^{(1)} + \vec{\sigma}^{(2)} \right) \cdot \vec{q} \right\}, \quad (71)$$

where we redefined \bar{g}_1 to absorb the tadpole contribution $\bar{g}_1 \rightarrow \bar{g}_1 + 2\bar{g}_0 \Delta m_N \delta m_\pi^2 / \delta m_N m_\pi^2$. The first structure contributes to 1S_0 - 3P_0 mixing. Being proportional to I_3 , the contribution vanishes in the case of neutron-proton scattering, and is only relevant for proton-proton or neutron-neutron scattering. Because of its isospin structure, it does not affect the 3S_1 - 1P_1 and 3S_1 - 3P_1 channels, and, in particular, it is not relevant for the calculation of the deuteron EDM. The second structure, in contrast, contributes to 3S_1 - 3P_1 mixing, and, consequently, to the deuteron EDM. Its contribution vanishes in the other low-energy channels.

Note that loop diagrams involving the leading S -wave TC four-nucleon operators and a TV pion exchange all vanish. The analysis of Refs. [67, 68] showed that some higher-wave TC four-nucleon operators are less suppressed than expected on the grounds of naive dimensional analysis, and they must be included in the leading-order $f = 4$ TC Lagrangian. Loop diagrams with P -wave operators and a TV pion exchange do not vanish. However, these diagrams do not depend on the momentum transfer \vec{q} and they simply renormalize the couplings \bar{C}_1 and \bar{C}_2 .

One can proceed in the same manner to construct higher-order potentials. At next order there are further OPE and TPE, and also one-photon-exchange, contributions to the two-nucleon potential. There is also the appearance of the lowest-order three-nucleon TV potential, which arises from essentially three mechanisms: (i) a TPE component $\propto g_A \bar{g}_0 / m_N F_\pi^4$ involving a pion energy in a Weinberg-Tomozawa seagull vertex; (ii) a TPE component $\propto g_A^2 \bar{h}_0 / F_\pi^4$ involving the seagull vertex from $\mathcal{L}_{f=2,T4}^{(2)}$, Eq. (23); and (iii) a one-pion/short-range component $\propto g_A \bar{\gamma}_i / F_\pi^2$ involving the short-range pion-two-nucleon interactions from $\mathcal{L}_{f=4,T4}^{(2)}$, Eq. (25). The fact that, in the absence of an explicit delta isobar, the three-nucleon potential first shows up three orders beyond leading is completely analogous to the TC PC case [50]. An important difference is that, because of the relative enhancement of pion exchange compared to short-range physics, the leading TV PV three-nucleon force does not include a purely short-range component. Thus, this TV PV three-nucleon force is in principle determined by one- and two-nucleon physics.

4.2 Dimension-6 Sources

Our attention has been focused so far on the TV potential from the $\bar{\theta}$ term, in which case the vanishing of \bar{g}_1 at leading order makes it important to consider subleading contributions. We now briefly turn our attention to the TV potential from dimension-6 sources of T violation.

For all dimension-6 sources, the leading-order potential contains OPE of the form in Fig. 2. Since these sources all generate $I = 0$ and $I = 1$ pion-nucleon couplings of the same size, we have no motivation to go to subleading order in the potential. The leading-order potential, which is a function of the transfer momentum \vec{q} only, should be sufficient for most phenomenological applications. Of course, if needed, subleading orders can be derived just as we have done for $\bar{\theta}$.

In the case of the qCEDM, the TV couplings \bar{g}_0 and \bar{g}_1 both appear in the $\Delta = -1$ Lagrangian, Eq. (39). As a consequence, the leading potential from the qCEDM has chiral index $\nu = -1$, and it has both an isospin-conserving part, which is identical to Eq. (55), and an isospin-breaking one. The leading

potential is

$$\begin{aligned}
V_{\text{qCEDM}}^{(-1)}(\vec{q}) &= i \frac{g_A \bar{g}_0}{F_\pi^2} \vec{\tau}^{(1)} \cdot \vec{\tau}^{(2)} \left(\vec{\sigma}^{(1)} - \vec{\sigma}^{(2)} \right) \cdot \frac{\vec{q}}{\vec{q}^2 + m_\pi^2} \\
&+ i \frac{g_A \bar{g}_1}{2F_\pi^2} \left[\left(\tau_3^{(1)} + \tau_3^{(2)} \right) \left(\vec{\sigma}^{(1)} - \vec{\sigma}^{(2)} \right) + \left(\tau_3^{(1)} - \tau_3^{(2)} \right) \left(\vec{\sigma}^{(1)} + \vec{\sigma}^{(2)} \right) \right] \cdot \frac{\vec{q}}{\vec{q}^2 + m_\pi^2}. \quad (72)
\end{aligned}$$

For the TV chiral-invariant (CI) sources, that is, gCEDM and TV FQ, the $\Delta = -1$ TV Lagrangian contains both pion-nucleon couplings and four-nucleon operators, see Eqs. (39) and (41). The additional TV pion-nucleon coupling \bar{t}_1 produces a potential of the type (70), and thus can be absorbed in redefinitions $\bar{g}_0 \rightarrow \bar{g}_0 + m_\pi^2 \bar{t}_1$ and $\bar{C}_2 \rightarrow \bar{C}_2 + 2g_A \bar{t}_1 / F_\pi^2$. As a consequence, the leading two-nucleon potential consists of an isospin-conserving and an isospin-breaking one-pion-exchange contribution and a short-distance piece,

$$\begin{aligned}
V_{\text{TVCI}}^{(-1)}(\vec{q}) &= i \frac{g_A \bar{g}_0}{F_\pi^2} \vec{\tau}^{(1)} \cdot \vec{\tau}^{(2)} \left(\vec{\sigma}^{(1)} - \vec{\sigma}^{(2)} \right) \cdot \frac{\vec{q}}{\vec{q}^2 + m_\pi^2} \\
&+ i \frac{g_A \bar{g}_1}{2F_\pi^2} \left[\left(\tau_3^{(1)} + \tau_3^{(2)} \right) \left(\vec{\sigma}^{(1)} - \vec{\sigma}^{(2)} \right) + \left(\tau_3^{(1)} - \tau_3^{(2)} \right) \left(\vec{\sigma}^{(1)} + \vec{\sigma}^{(2)} \right) \right] \cdot \frac{\vec{q}}{\vec{q}^2 + m_\pi^2} \\
&- \frac{i}{2} \left[\bar{C}_1 + \bar{C}_2 \vec{\tau}^{(1)} \cdot \vec{\tau}^{(2)} \right] \left(\vec{\sigma}^{(1)} - \vec{\sigma}^{(2)} \right) \cdot \vec{q}. \quad (73)
\end{aligned}$$

The qEDM leading-order potential displays further new structures: in addition to the $I = 2$ pion-nucleon coupling \bar{g}_2 in Eq. (39), there is also the one-photon-exchange contribution shown in Fig. 1, where one vertex is the short-distance contribution (40) to the nucleon EDM:

$$\begin{aligned}
V_{\text{qEDM}}^{(2)}(\vec{q}) &= i \frac{g_A}{F_\pi^2} \left(\bar{g}_0 \vec{\tau}^{(1)} \cdot \vec{\tau}^{(2)} + \bar{g}_2 \tau_3^{(1)} \tau_3^{(2)} \right) \left(\vec{\sigma}^{(1)} - \vec{\sigma}^{(2)} \right) \cdot \frac{\vec{q}}{\vec{q}^2 + m_\pi^2} \\
&+ i \frac{g_A \bar{g}_1}{2F_\pi^2} \left[\left(\tau_3^{(1)} + \tau_3^{(2)} \right) \left(\vec{\sigma}^{(1)} - \vec{\sigma}^{(2)} \right) + \left(\tau_3^{(1)} - \tau_3^{(2)} \right) \left(\vec{\sigma}^{(1)} + \vec{\sigma}^{(2)} \right) \right] \cdot \frac{\vec{q}}{\vec{q}^2 + m_\pi^2} \\
&- i \frac{e}{2} \left(\bar{d}_0 + \bar{d}_1 \tau_3^{(1)} \tau_3^{(2)} \right) \left(\vec{\sigma}^{(1)} - \vec{\sigma}^{(2)} \right) \cdot \frac{\vec{q}}{\vec{q}^2} \\
&- i \frac{e}{4} \left[\left(\bar{d}_0 + \bar{d}_1 \right) \left(\tau_3^{(1)} + \tau_3^{(2)} \right) \left(\vec{\sigma}^{(1)} - \vec{\sigma}^{(2)} \right) + \left(\bar{d}_1 - \bar{d}_0 \right) \left(\tau_3^{(1)} - \tau_3^{(2)} \right) \left(\vec{\sigma}^{(1)} + \vec{\sigma}^{(2)} \right) \right] \cdot \frac{\vec{q}}{\vec{q}^2}. \quad (74)
\end{aligned}$$

As for $\bar{\theta}$, at subleading orders the potential receives corrections from various mechanisms. For all dimension-6 sources there are one-loop diagrams with the same topology as in Fig. 3, the square now denoting \bar{g}_0 , \bar{g}_1 or \bar{g}_2 . There are also tree-level OPE diagrams of the type in Fig. 4, with subleading TC and TV pion-nucleon vertices. For qCEDM and qEDM, the one-derivative four-nucleon interactions in the Lagrangian (42) have to be taken into account, while for TV CI sources one has to include all the possible TV four-nucleon operators with three derivatives. For qEDM, one also needs to include corrections involving photon exchange. This calculation proceeds along lines that are very similar to Sect. 4.1.

In the case of the $\bar{\theta}$ term, TV three-nucleon forces only appear at NNNLO, one order higher than the accuracy of our analysis. For qCEDM and qEDM the situation is similar, but one might wonder whether for CI sources, which appear to be more sensitive to short-distance physics, TV three-nucleon forces are more relevant. However, also in this case it turns out that the three-nucleon potential is a NNNLO effect. The lowest-order three-nucleon potential receives various contributions: (i) a TPE component $\propto g_A \bar{g}_{0,1} / m_N F_\pi^4$ involving a pion energy in the Weinberg-Tomozawa vertex; (ii) a TPE component $\propto g_A^2 \bar{t}_0 / m_N F_\pi^4$ involving a pion energy in the leading TV seagull \bar{t}_0 ; (iii) TPE components from TV seagulls in the $\Delta = 0$ pion-nucleon Lagrangian, which we did not explicitly construct; (iv) a one-pion/short-range component $\propto g_A \bar{\gamma}_i / F_\pi^2$, with four-nucleon operators that contain at least one pion

field in the $\Delta = 0$ Lagrangian; and (v) short-range six-nucleon operators, which also appear in the $\Delta = 0$ Lagrangian. From the power counting formula (13), all these three-nucleon contributions are suppressed by three powers of Q/M_{QCD} with respect to the effects of the two-nucleon potential (73) in the three-body system.

5 The TV Potential in Configuration Space

The evaluation of T -odd observables in nuclear and atomic systems is often more easily carried out in configuration space. In this section we give the TV nuclear potential derived in Sect. 4 in coordinate space. We compare this potential with the literature in the next section.

In the two-body case, it is convenient to introduce the relative position of the two nucleons $\vec{r} = \vec{x}_1 - \vec{x}_2$, their CM coordinate $\vec{X} = (\vec{x}_1 + \vec{x}_2)/2$, and the conjugate variables $-i\vec{\nabla}_r \equiv -i\partial/\partial\vec{r}$ and $-i\vec{\nabla}_X \equiv -i\partial/\partial\vec{X}$. Translation invariance constrains the potential to commute with $\vec{\nabla}_X$ and, therefore, not to depend on \vec{X} , so that in general the potential is a function of \vec{r} and of the nucleons' relative and CM momenta, $V_T = V_T(\vec{r}, \vec{\nabla}_r, \vec{\nabla}_X)$. The relations between the potential in momentum space and in coordinate space are detailed in the Appendix. Some care must be taken, and a regularization scheme has to be defined, when computing the Fourier transform of functions that blow up as $|\vec{q}|$ goes to infinity, as is the case of the subleading TV potential. As described in the Appendix, we follow Ref. [82] and define the Fourier transform in d dimensions. We apply the d -dimensional Fourier integration of the momentum-space potential before setting $d = 4$. This method eliminates naturally the divergent factor $\Gamma(2 - d/2)$ arising from loops and yields a finite result. As we will see, the divergent behavior at large momentum translates in a singular $\sim 1/r^4$ potential at short distances. Expressions in configuration space obtained with this method are equivalent to the procedure based on old-fashioned perturbation theory [82].

In order to write the results of the Fourier transform we introduce a few functions of the magnitude $r = |\vec{r}|$ of the radial coordinate:

$$U(r) = \frac{1}{12\pi r} [2 \exp(-m_{\pi^\pm} r) + \exp(-m_{\pi^0} r)], \quad (75)$$

which reduces to the usual Yukawa function $U(r) = \exp(-m_\pi r)/4\pi r$ when we ignore the pion mass difference;

$$W(r) = \frac{1}{4\pi r} [\exp(-m_{\pi^\pm} r) - \exp(-m_{\pi^0} r)], \quad (76)$$

which is entirely a consequence of isospin breaking; and the TPE functions

$$X(r) = \frac{1}{4\pi(2\pi F_\pi)^2 r^3} \int_0^1 dx (3 + 3\beta r + \beta^2 r^2) \exp(-\beta r), \quad (77)$$

$$Y(r) = \frac{1}{2\pi(2\pi F_\pi)^2 r^3} \int_0^1 dx (1 + \beta r) \exp(-\beta r), \quad (78)$$

with $\beta^2 = m_\pi^2/x(1-x)$.

5.1 $\bar{\theta}$ Term

The Fourier transform of the leading OPE potential including the corrections from the pion mass (64) and from the nucleon kinetic energy (66), is

$$V_\theta^{(1)}(\vec{r}) + V_{\theta,a}^{(2+3)}(\vec{r}) + V_{\theta,c}^{(3)}(\vec{r}, \vec{\nabla}_r, \vec{\nabla}_X) = -\frac{\bar{g}_0 g_A}{F_\pi^2} \vec{\tau}^{(1)} \cdot \vec{\tau}^{(2)} \left(\vec{\sigma}^{(1)} - \vec{\sigma}^{(2)} \right) \cdot \left[\left(\vec{\nabla}_r U(r) \right) \left(1 + \frac{\vec{\nabla}_X^2}{4m_N^2} \right) + \left\{ \frac{\nabla_r^i}{2m_N}, \left\{ \frac{\nabla_r^i}{2m_N}, \left(\vec{\nabla}_r U(r) \right) \right\} \right\} + \frac{(\vec{\nabla}_r \cdot \vec{\nabla}_X)^2}{8m_\pi m_N^2} \left(\vec{\nabla}_r r U(r) \right) \right], \quad (79)$$

where $\{\cdots, \cdots\}$ denotes the anticommutator. The remaining pion-mass correction, Eq. (65), is

$$V_{\bar{\theta},b}^{(2+3)}(\vec{r}) = \frac{\bar{g}_0 g_A}{3F_\pi^2} \left(3\tau_3^{(1)} \tau_3^{(2)} - \vec{\tau}^{(1)} \cdot \vec{\tau}^{(2)} \right) \left(\vec{\sigma}^{(1)} - \vec{\sigma}^{(2)} \right) \cdot \left(\vec{\nabla}_r U(r) \right), \quad (80)$$

while the Fourier transform of the other relativistic corrections to the leading OPE, Eq. (67), is

$$\begin{aligned} V_{\bar{\theta},d}^{(3)}(\vec{r}, \vec{\nabla}_r, \vec{\nabla}_X) &= -\frac{\bar{g}_0 g_A}{8F_\pi^2 m_N^2} \vec{\tau}^{(1)} \cdot \vec{\tau}^{(2)} \left[\left(\vec{\sigma}^{(1)} - \vec{\sigma}^{(2)} \right) \cdot \vec{\nabla}_X \left(\vec{\nabla}_r U(r) \right) \cdot \vec{\nabla}_X \right. \\ &\quad + \left(\vec{\sigma}^{(1)} + \vec{\sigma}^{(2)} \right) \cdot \left\{ \vec{\nabla}_r, \left(\vec{\nabla}_r U(r) \right) \cdot \vec{\nabla}_X \right\} \\ &\quad + 2i\varepsilon^{ijk} \left(\sigma^{(1)i} \sigma^{(2)l} - \sigma^{(1)l} \sigma^{(2)i} \right) \left(\nabla_r^l \nabla_r^k U(r) \right) \nabla_r^j \\ &\quad \left. + i\varepsilon^{ijk} \left(\sigma^{(1)i} \sigma^{(2)l} + \sigma^{(1)l} \sigma^{(2)i} \right) \left(\nabla_r^l \nabla_r^k U(r) \right) \nabla_X^j \right]. \end{aligned} \quad (81)$$

The nucleon mass-splitting corrections in Eq. (68) become

$$\begin{aligned} V_{\bar{\theta},e}^{(3)}(\vec{r}, \vec{\nabla}_r, \vec{\nabla}_X) &= -i\frac{\bar{g}_0 g_A}{2F_\pi^2} \frac{\delta m_N}{m_N} \left(\vec{\tau}^{(1)} \times \vec{\tau}^{(2)} \right)_3 \left[\left(\vec{\sigma}^{(1)} + \vec{\sigma}^{(2)} \right) \cdot \left\{ \vec{\nabla}_r, U(r) \right\} \right. \\ &\quad \left. + \left(\vec{\sigma}^{(1)} - \vec{\sigma}^{(2)} \right) \cdot \left(U(r) \vec{\nabla}_X - \frac{1}{m_\pi} \left(\vec{\nabla}_r \nabla_r^i U(r) \right) \nabla_X^i \right) \right], \end{aligned} \quad (82)$$

while those in Eq. (69) read

$$V_{\bar{\theta},f}^{(3)}(\vec{r}) = -\frac{\bar{g}_0 g_A}{3F_\pi^2} \frac{\delta m_N^2}{m_\pi} \left[\vec{\tau}^{(1)} \cdot \vec{\tau}^{(2)} - \frac{1}{2} \left(3\tau_3^{(1)} \tau_3^{(2)} - \vec{\tau}^{(1)} \cdot \vec{\tau}^{(2)} \right) \right] \left(\vec{\sigma}^{(1)} - \vec{\sigma}^{(2)} \right) \cdot \left(\vec{\nabla}_r U(r) \right). \quad (83)$$

The last OPE terms, Eq. (71), are

$$\begin{aligned} V_{\bar{\theta},g}^{(3)}(\vec{r}) &= -\frac{\bar{g}_0 g_A}{2F_\pi^2} \left[\left(\frac{\bar{g}_1}{\bar{g}_0} - \frac{\beta_1}{2g_A} \right) \left(\tau_3^{(1)} + \tau_3^{(2)} \right) \left(\vec{\sigma}^{(1)} - \vec{\sigma}^{(2)} \right) \right. \\ &\quad \left. + \left(\frac{\bar{g}_1}{\bar{g}_0} + \frac{\beta_1}{2g_A} \right) \left(\tau_3^{(1)} - \tau_3^{(2)} \right) \left(\vec{\sigma}^{(1)} + \vec{\sigma}^{(2)} \right) \right] \cdot \left(\vec{\nabla}_r U(r) \right). \end{aligned} \quad (84)$$

Finally, the Fourier transform of the TPE potential in Eq. (60) reads

$$V_{\bar{\theta},MR}^{(3)}(\vec{r}) = -\frac{\bar{g}_0 g_A}{F_\pi^2} \vec{\tau}^{(1)} \cdot \vec{\tau}^{(2)} \left(\vec{\sigma}^{(1)} - \vec{\sigma}^{(2)} \right) \cdot \left[\vec{\nabla}_r \left(2g_A^2 X(r) - Y(r) \right) \right]. \quad (85)$$

The potential in Eq. (85) is singular, and the cutoff dependence it introduces in the evaluation of matrix elements and observables is absorbed by the renormalization of \bar{C}_2 in the short-distance potential (59),

$$V_{\bar{\theta},SR}^{(3)}(\vec{r}) = \frac{1}{2} \left[\bar{C}_1 + \bar{C}_2 \vec{\tau}^{(1)} \cdot \vec{\tau}^{(2)} \right] \left(\vec{\sigma}^{(1)} - \vec{\sigma}^{(2)} \right) \cdot \left(\vec{\nabla}_r \delta^{(3)}(\vec{r}) \right). \quad (86)$$

5.2 Dimension-6 Sources

At leading order, the potential from dimension-6 sources is local, and depends only on the relative position \vec{r} .

In the case of the qCEDM, since the potential arises from one-pion exchange, its radial dependence is encoded in the Yukawa function $U(r)$,

$$\begin{aligned} V_{\text{qCEDM}}^{(-1)}(\vec{r}) &= -\frac{\bar{g}_0 g_A}{F_\pi^2} \vec{\tau}^{(1)} \cdot \vec{\tau}^{(2)} \left(\vec{\sigma}^{(1)} - \vec{\sigma}^{(2)} \right) \cdot \left(\vec{\nabla}_r U(r) \right) \\ &\quad - \frac{\bar{g}_1 g_A}{2F_\pi^2} \left[\left(\tau_3^{(1)} + \tau_3^{(2)} \right) \left(\vec{\sigma}^{(1)} - \vec{\sigma}^{(2)} \right) + \left(\tau_3^{(1)} - \tau_3^{(2)} \right) \left(\vec{\sigma}^{(1)} + \vec{\sigma}^{(2)} \right) \right] \cdot \left(\vec{\nabla}_r U(r) \right). \end{aligned} \quad (87)$$

For CI sources, there are additional short-range contributions,

$$\begin{aligned}
V_{\text{TVCI}}^{(-1)}(\vec{r}) &= -\frac{\bar{g}_0 g_A}{F_\pi^2} \vec{\tau}^{(1)} \cdot \vec{\tau}^{(2)} \left(\vec{\sigma}^{(1)} - \vec{\sigma}^{(2)} \right) \cdot \left(\vec{\nabla}_r U(r) \right) \\
&\quad - \frac{\bar{g}_1 g_A}{2F_\pi^2} \left[\left(\tau_3^{(1)} + \tau_3^{(2)} \right) \left(\vec{\sigma}^{(1)} - \vec{\sigma}^{(2)} \right) + \left(\tau_3^{(1)} - \tau_3^{(2)} \right) \left(\vec{\sigma}^{(1)} + \vec{\sigma}^{(2)} \right) \right] \cdot \left(\vec{\nabla}_r U(r) \right) \\
&\quad + \frac{1}{2} \left[\bar{C}_1 + \bar{C}_2 \vec{\tau}^{(1)} \cdot \vec{\tau}^{(2)} \right] \left(\vec{\sigma}^{(1)} - \vec{\sigma}^{(2)} \right) \cdot \left(\vec{\nabla}_r \delta^{(3)}(\vec{r}) \right). \tag{88}
\end{aligned}$$

The potential from the qEDM is purely long-distance: in addition to pion exchange of range $\sim 1/m_\pi$, there is a longer-range component from photon exchange,

$$\begin{aligned}
V_{\text{qEDM}}^{(2)}(\vec{r}) &= -\frac{g_A}{F_\pi^2} \left(\bar{g}_0 \vec{\tau}^{(1)} \cdot \vec{\tau}^{(2)} + \bar{g}_2 \tau_3^{(1)} \tau_3^{(2)} \right) \left(\vec{\sigma}^{(1)} - \vec{\sigma}^{(2)} \right) \cdot \left(\vec{\nabla}_r U(r) \right) \\
&\quad - \frac{\bar{g}_1 g_A}{2F_\pi^2} \left[\left(\tau_3^{(1)} + \tau_3^{(2)} \right) \left(\vec{\sigma}^{(1)} - \vec{\sigma}^{(2)} \right) + \left(\tau_3^{(1)} - \tau_3^{(2)} \right) \left(\vec{\sigma}^{(1)} + \vec{\sigma}^{(2)} \right) \right] \cdot \left(\vec{\nabla}_r U(r) \right) \\
&\quad + \frac{e}{2} \left[\bar{d}_0 + \bar{d}_1 \tau_3^{(1)} \tau_3^{(2)} \right] \left(\vec{\sigma}^{(1)} - \vec{\sigma}^{(2)} \right) \cdot \left(\vec{\nabla}_r \frac{1}{4\pi r} \right) \\
&\quad + \frac{e}{4} \left[(\bar{d}_0 + \bar{d}_1) \left(\tau_3^{(1)} + \tau_3^{(2)} \right) \left(\vec{\sigma}^{(1)} - \vec{\sigma}^{(2)} \right) + (\bar{d}_1 - \bar{d}_0) \left(\tau_3^{(1)} - \tau_3^{(2)} \right) \left(\vec{\sigma}^{(1)} + \vec{\sigma}^{(2)} \right) \right] \\
&\quad \cdot \left(\vec{\nabla}_r \frac{1}{4\pi r} \right). \tag{89}
\end{aligned}$$

The various sources thus involve different spin, isospin, and radial dependences. We discuss some implications in the next section.

6 Discussion

Traditionally the study on T violation in nuclear physics has been carried out by considering the most general pion-nucleon *non*-derivative couplings in a phenomenological TV Lagrangian [31], which we write in our notation as

$$\mathcal{L}_{T,\text{non}} = -\frac{\bar{g}_0}{F_\pi} \bar{N} \vec{\tau} \cdot \vec{\pi} N - \frac{\bar{g}_1}{F_\pi} \pi_3 \bar{N} N - \frac{\bar{g}_2}{F_\pi} \pi_3 \bar{N} \tau_3 N, \tag{90}$$

and by inferring from it the TV two-nucleon potential [30],

$$\begin{aligned}
V_{T,\text{non}}(\vec{r}) &= -\frac{g_A}{F_\pi^2} \left\{ \left[\left(\bar{g}_0 + \frac{\bar{g}_2}{3} \right) \vec{\tau}^{(1)} \cdot \vec{\tau}^{(2)} + \frac{\bar{g}_1}{2} \left(\tau_3^{(1)} + \tau_3^{(2)} \right) + \frac{\bar{g}_2}{3} \left(3\tau_3^{(1)} \tau_3^{(2)} - \vec{\tau}^{(1)} \cdot \vec{\tau}^{(2)} \right) \right] \right. \\
&\quad \left. \left(\vec{\sigma}^{(1)} - \vec{\sigma}^{(2)} \right) + \frac{\bar{g}_1}{2} \left(\tau_3^{(1)} - \tau_3^{(2)} \right) \left(\vec{\sigma}^{(1)} + \vec{\sigma}^{(2)} \right) \right\} \cdot \left(\vec{\nabla} U(r) \right), \tag{91}
\end{aligned}$$

with $U(r)$ defined in Eq. (75). When short-distance contributions are included in the model, the most general TV two-nucleon local potential with the *minimum* number of derivatives assumes the form [35]

$$\begin{aligned}
V_{T,\text{min}}(\vec{r}) &= \left(\vec{\sigma}^{(1)} - \vec{\sigma}^{(2)} \right) \cdot \vec{\nabla} \left[\mathcal{U}_0(r) + \vec{\tau}^{(1)} \cdot \vec{\tau}^{(2)} \mathcal{V}_0(r) + \frac{1}{2} \left(\tau_3^{(1)} + \tau_3^{(2)} \right) \mathcal{U}_1(r) \right. \\
&\quad \left. + \left(3\tau_3^{(1)} \tau_3^{(2)} - \vec{\tau}^{(1)} \cdot \vec{\tau}^{(2)} \right) \mathcal{V}_2(r) \right] + \frac{1}{2} \left(\tau_3^{(1)} - \tau_3^{(2)} \right) \left(\vec{\sigma}^{(1)} + \vec{\sigma}^{(2)} \right) \cdot \vec{\nabla} \mathcal{V}_1(r) \tag{92}
\end{aligned}$$

in terms of five radial functions $\mathcal{U}_{0,1}(r)$ and $\mathcal{V}_{0,1,2}(r)$. These functions are assumed to originate in one-boson exchange [32, 33, 34]: pion exchange is taken to give long-range contributions to \mathcal{V}_0 , $(\mathcal{V}_1 + \mathcal{U}_1)/2$ and \mathcal{V}_2 , while eta, rho and omega mesons give shorter-range contributions to the same quantities, and to \mathcal{U}_0 and $\mathcal{V}_1 - \mathcal{U}_1$. The five momentum-independent potentials in Eq. (92) are treated on the same footing, and they provide enough information to describe the five S - P mixing amplitudes discussed in Sect. 3.

For TV stemming from the QCD $\bar{\theta}$ term, the proper account of chiral symmetry radically changes the picture. As noticed in Ref. [20], at leading order the $\bar{\theta}$ term generates only the isoscalar pion-nucleon T -odd coupling \bar{g}_0 , and thus contributes at tree level only to the $I = 0$ potential [29]. A coupling of \bar{g}_1 form appears two orders down in the ChPT expansion, and the one of \bar{g}_2 form is even more suppressed [25]. To evaluate the effects of the $\bar{\theta}$ term on observables which, like the deuteron EDM, are mostly sensitive to the $I = 1$ components, it is necessary to consider the TV two-nucleon potential to next-to-next-to-leading order in ChPT. As described in Sect. 4, this implies the consideration not only of the non-derivative pion-nucleon TV couplings, but also of subleading TV derivative couplings, of power-suppressed TC interactions (with particular care for isospin-breaking operators, which contribute to the $I = 1$ and $I = 2$ potentials), and of one-loop and short-range contributions to the two-nucleon potential. When all these elements are considered, the potential has a much richer structure than Eq. (92): (i) a hierarchy emerges between the five spin-isospin structures already present in Eq. (92), and (ii) momentum-dependent potentials appear, with the same importance as most of the momentum-independent ones.

We first analyze the implications of our $\bar{\theta}$ results to $V_{T,\min}(\vec{r})$. Using the chiral index ν , as defined in Eq. (13), to keep track of the size of different pieces, the $\bar{\theta}$ contributions to Eq. (92) are

$$\mathcal{V}_0^{(1)}(r) = -\frac{g_A \bar{g}_0}{F_\pi^2} U(r), \quad (93)$$

$$\mathcal{V}_0^{(3)}(r) = -\frac{g_A \bar{g}_0}{F_\pi^2} \left[2g_A^2 X(r) - Y(r) + \frac{(m_n - m_p)^2}{3m_\pi} r U(r) \right] + \bar{C}_2 \frac{\delta(r)}{8\pi r^2}, \quad (94)$$

$$\mathcal{U}_0^{(3)}(r) = +\bar{C}_1 \frac{\delta(r)}{8\pi r^2}, \quad (95)$$

$$\mathcal{V}_1^{(3)}(r) = -\frac{g_A \bar{g}_0}{F_\pi^2} \left(\frac{\bar{g}_1}{\bar{g}_0} + \frac{\beta_1}{2g_A} \right) U(r), \quad (96)$$

$$\mathcal{U}_1^{(3)}(r) = -\frac{g_A \bar{g}_0}{F_\pi^2} \left(\frac{\bar{g}_1}{\bar{g}_0} - \frac{\beta_1}{2g_A} \right) U(r), \quad (97)$$

$$\mathcal{V}_2^{(2+3)}(r) = +\frac{g_A \bar{g}_0}{3F_\pi^2} \left[\frac{(m_n - m_p)^2}{2m_\pi} r U(r) + W(r) \right], \quad (98)$$

where $U(r)$, $W(r)$, $X(r)$, and $Y(r)$ are defined in Eqs. (75), (76), (77), and (78), respectively. In Eq. (93) the use of the definition (75) to express $\mathcal{V}_0^{(1)}$ in terms of the physical pion masses introduces subleading corrections in the $\nu = 1$ term, which strictly speaking would use a function $U(r)$ that only depends on a common pion mass, say the neutral one, $U_0(r) = \exp(-m_{\pi^0} r)/4\pi r$. In Eqs. (94)–(98) we can neglect the pion mass difference in $U(r)$, and use $U_0(r)$, the error thus introduced being at higher orders in the ChPT power counting. Similarly, in Eq. (93) the use of g_A and \bar{g}_0 with their m_π^2 corrections included accounts for some $\nu = 3$ corrections, while whether or not such m_π^2 corrections are included in Eqs. (94)–(98) is beyond the order we consider. In Eqs. (94) and (98) we replaced δm_N , the quark-mass-difference contribution to the nucleon mass splitting, with the physical value of the nucleon mass splitting itself, $m_n - m_p$, the difference again being a higher-order contribution in ChPT.

As one can see, at order $\nu = 3$ in ChPT all the possible spin-isospin structures considered in Refs. [35, 32, 33, 34] appear. The dominant component is the isoscalar \mathcal{V}_0 [29]. In Figs. 5 and 6 we plot, respectively, the momentum-space and configuration-space expressions for $\nabla \mathcal{V}_0$. The dashed line represents the leading-order $\nabla \mathcal{V}_0^{(1)}$, Eqs. (64) and (79) with the use of the definition (75) for $U(r)$ to express $\mathcal{V}_0^{(1)}$ in terms of the physical pion masses. The dashed-double-dotted line illustrates the effect of the difference between the leading OPE potential computed with the function $U(r)$ and with $U_0(r)$. Other isospin-breaking corrections, which come from the nucleon mass splitting in $\mathcal{V}_0^{(3)}$, Eqs. (69) and (83), are very small, as indicated by the long-dashed-dotted line barely distinguishable from the x -axis. At next-to-next-to-leading order, \mathcal{V}_0 also exhibits a medium-range component originating in TPE diagrams and a short-range component. The dashed-dotted line depicts the non-analytic piece of the TPE diagrams, Eqs. (60) and (85). We estimate the short-range potential by assuming the coefficient \bar{C}_2 in Eq. (58) to be dominated by the $\ln \mu^2/m_\pi^2$ term with $\mu = m_N$. The rationale is that there is no obvious reason

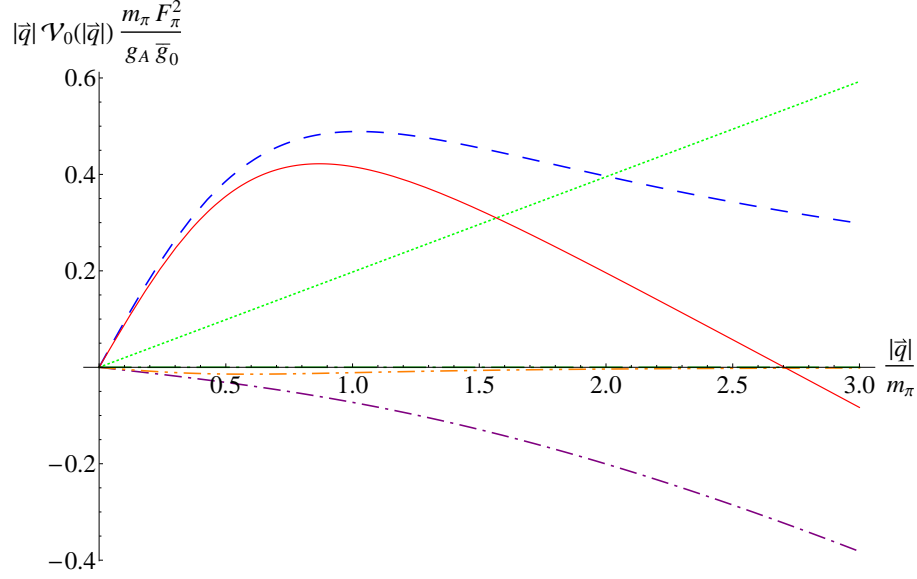


Figure 5: Components of the $\bar{\theta}$ -term two-nucleon potential $|\vec{q}|\mathcal{V}_0$, in units of $g_A\bar{g}_0/F_\pi^2 m_\pi$, as a function of the transferred momentum $|\vec{q}|$, in units of m_π . The (blue) dashed line denotes the leading-order OPE contribution with physical pion masses; the (orange) dashed-double-dotted line shows the effect of the pion mass difference on the leading OPE contribution; the (dark green) long-dashed-dotted line accounts for the even smaller effect of the nucleon mass splitting; the (purple) dashed-dotted line is the non-analytic TPE contribution; and the (green) dotted line presents an estimate of the short-range component of the potential. The (red) solid line is the sum of all contributions up to next-to-next-to-leading order, except for the short-range component.

to expect that such a contribution, non-analytic in m_π , should get exactly canceled by m_π -independent short-distance contributions. However, the sign cannot be guessed reliably and our choice is purely arbitrary, for illustration only. Equation (59) gives rise to the straight dotted line in Fig. 5 but Eq. (86) does not appear in Fig. 6 since it is concentrated at $r = 0$. The solid line in both figures is the sum of the long and medium range contributions to $\nabla\mathcal{V}_0$.

From Fig. 5, we can appreciate that, as expected from the ChPT power counting, the medium and short-range corrections to the TV potential have comparable size in the momentum range we are considering, and for momenta $q \gtrsim m_\pi$ they noticeably affect the leading order. At momenta of order 300–400 MeV the medium and short-range contributions have roughly the same size as the leading potential. In this region, degrees of freedom which we have not explicitly included in the EFT, like the Δ isobar, become relevant, and the convergence of the perturbative expansion can be improved by extending the EFT to incorporate them. Isospin-breaking, long-range corrections, although of formally the same order as TPE and contact terms, are much smaller, at least in part because of factors of ε , except at very small momenta where their longer range compensates. In Fig. 6 we focus our attention on the long-distance region, $r \geq 1/m_\pi$. At distances of up to $r \lesssim 2/m_\pi$ TPE is still the dominant correction to the potential, but it is overcome at longer distances, $r \gtrsim 2/m_\pi$, by the long-range effects of pion mass splitting in OPE.

It is instructive to compare our results for \mathcal{V}_0 to the corresponding TV potential obtained in a one-boson-exchange model. In such a model, T violation in the coupling of a rho meson to the nucleon generates corrections to \mathcal{V}_0 of the form [33, 34]

$$\mathcal{V}_0^{(\rho)}(r) = -\frac{g_A\bar{g}_0}{F_\pi^2} \frac{g_{\rho NN}}{g_{\pi NN}} \frac{\bar{g}_{0\rho}F_\pi}{\bar{g}_0} \frac{e^{-m_\rho r}}{4\pi r}, \quad (99)$$

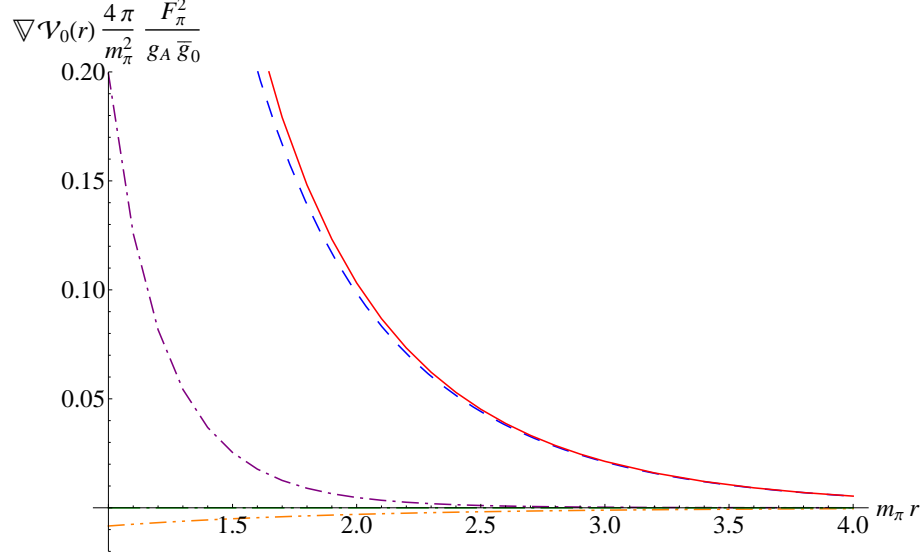


Figure 6: Components of the $\bar{\theta}$ -term two-nucleon potential $\nabla \mathcal{V}_0$ in units of $g_A \bar{g}_0 m_\pi^2 / 4\pi F_\pi^2$, as functions of the distance between the two nucleons $r = |\vec{r}|$, in units of $1/m_\pi$. Curves as in Fig. 5, except that the short-range component of the potential is not shown.

where $g_{\rho NN}$ is the TC rho-nucleon vector coupling and $\bar{g}_{0\rho}$ is an isoscalar, TV, one-derivative rho-nucleon coupling, defined, for example, in Ref. [34]. In the limit where the rho mass is large, $m_\rho \rightarrow \infty$, $\mathcal{V}_0^{(\rho)}(r)$ approximates a delta function and the effect of TV rho-exchange amounts to a contribution to \bar{C}_2 of the form

$$\bar{C}_2^{(\rho)} = -2 \frac{g_A \bar{g}_0}{F_\pi^2} \frac{g_{\rho NN}}{g_{\pi NN}} \frac{\bar{g}_{0\rho} F_\pi}{\bar{g}_0} \frac{1}{m_\rho^2}. \quad (100)$$

Since $m_\rho \sim M_{QCD}$ and there is no reason for $\bar{g}_{0\rho} F_\pi / \bar{g}_0$ to be particularly big or small, the size of rho-meson contribution is comparable to the power-counting expectation, $\bar{C}_2 = \mathcal{O}(\theta m_\pi^2 / F_\pi^2 M_{QCD}^3)$, with some suppression coming from the numerical smallness of the TC rho-nucleon vector coupling compared to the pion-nucleon coupling. Assuming the TV pion-nucleon and rho-nucleon couplings to have the same strength, $\bar{g}_{0\rho} F_\pi / \bar{g}_0 = 1$, and using for the rho-nucleon vector coupling the value determined in modern high-precision two-nucleon potentials, $g_{\rho NN} = 3.2$ [83], in Fig. 7 we compare the rho-meson contribution to $\nabla \mathcal{V}_0$ to the pion-mass-splitting and TPE medium-range corrections discussed above. For $r \gtrsim 1/m_\pi$, the contribution of the rho meson is numerically small compared to both pion-mass-splitting and TPE corrections. At shorter ranges, $r \lesssim 1/m_\pi$, rho exchange overcomes the effect of pion mass splitting, but it always remains smaller than TPE. Of course we can make one-rho exchange more important by jacking up $\bar{g}_{0\rho} F_\pi / \bar{g}_0$, but we cannot compensate for the different ranges of the two contributions, m_ρ versus $2m_\pi$. We see little justification for neglecting TPE in the $\bar{\theta}$ potential.

We now turn to the other spin-isospin structures in Eq. (92), which in EFT are all suppressed by one power of Q^2/M_{QCD}^2 with respect to the leading OPE TV potential. The function $\mathcal{U}_0^{(3)}$ only receives contributions from short-range physics. Again, in a one-boson-exchange scenario, contributions of exactly the size of \bar{C}_1 come from eta and omega exchanges [32, 33, 34],

$$\bar{C}_1^{(\eta, \omega)} = 2 \frac{g_A \bar{g}_0}{F_\pi^2} \left(\frac{g_{\eta NN}}{g_{\pi NN}} \frac{\bar{g}_{0\eta} F_\pi}{\bar{g}_0} \frac{1}{m_\eta^2} - \frac{g_{\omega NN}}{g_{\pi NN}} \frac{\bar{g}_{0\omega} F_\pi}{\bar{g}_0} \frac{1}{m_\omega^2} \right), \quad (101)$$

where m_η (m_ω) is the eta (omega) mass, $g_{\eta NN}$ ($g_{\omega NN}$) is the TC eta-nucleon axial (omega-nucleon vector) coupling, and $\bar{g}_{0\eta}$ ($\bar{g}_{0\omega}$) is an isoscalar, TV no-derivative eta-nucleon (one-derivative omega-nucleon)

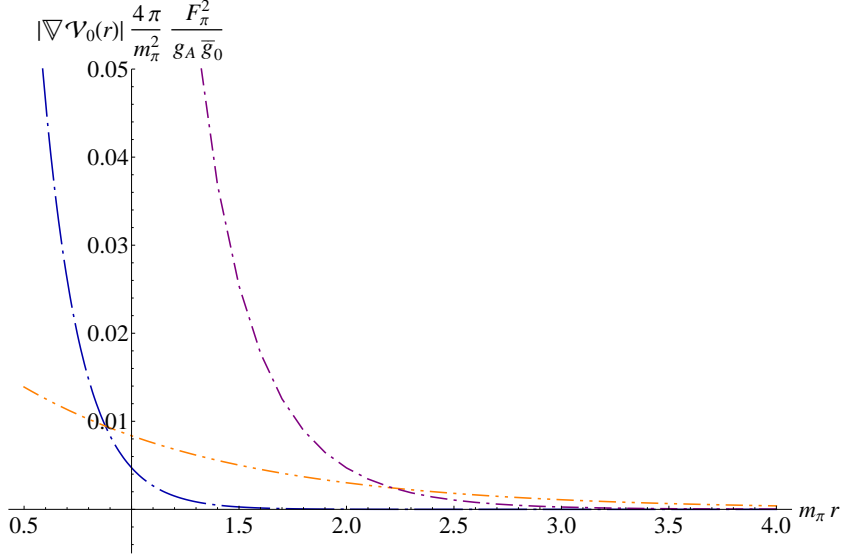


Figure 7: Comparison between one-rho-exchange and EFT contributions to the magnitude of the $\bar{\theta}$ potential $|\nabla\mathcal{V}_0|$ in units of $g_A\bar{g}_0m_\pi^2/4\pi F_\pi^2$, as functions of the distance r , in units of $1/m_\pi$. The rho-exchange contribution is depicted as a (blue) long-dashed-dotted line, while TPE and pion mass splitting in OPE are as in Fig. 5.

coupling. The eta- and omega-meson contributions are comparable to the power-counting expectation $\bar{C}_1 = \mathcal{O}(\bar{\theta}m_\pi^2/F_\pi^2 M_{QCD}^3)$. For the eta meson, the enhancement due to the relatively light mass is offset by the smallness of eta-nucleon TC coupling, $g_{\eta NN} = 2.24$ [84]. The ratio $g_{\omega NN}/g_{\pi NN}$ is instead close to one [83], and, therefore, we have no reason to expect the omega-meson contribution to \bar{C}_1 to differ much from the power-counting estimate.

In contrast, $\mathcal{V}_1^{(3)}$, $\mathcal{U}_1^{(3)}$, and $\mathcal{V}_2^{(2+3)}$ sprout entirely from OPE. The TV, isospin-breaking coupling \bar{g}_1 contributes equally to \mathcal{V}_1 and \mathcal{U}_1 , as expected [30] from the identification at the Lagrangian level, *cf.* Eqs. (24) and (90). However, we expect a comparable long-range piece in $\mathcal{U}_1 - \mathcal{V}_1$, which stems from the combination of the isospin-violating vertex β_1 and the TV vertex \bar{g}_0 . As discussed in Ref. [25], strong-dynamics contributions to the coefficients of these $I = 1$ potentials are in principle determined by measurement of TC, isospin-breaking observables. For example \bar{g}_1/\bar{g}_0 could be extracted from a detailed analysis of isospin-breaking effects in pion-nucleon scattering. At present, however, even the very sophisticated, state-of-the art analysis of Ref. [85] stops one order shy of the accuracy required for such extraction. Similarly, the ratio β_1/g_A affects isospin violation in nucleon-nucleon scattering, but at present phase-shift analyses of two-nucleon data can only provide a bound on β_1 , which is in accordance with the power-counting expectation [51, 52]. In the absence of better constraints on the parameters in Eqs. (96) and (97), the ratios $\mathcal{V}_1^{(3)}/\mathcal{V}_0^{(1)}$ and $\mathcal{U}_1^{(3)}/\mathcal{V}_0^{(1)}$ can only be estimated by power counting, as $\mathcal{O}(\varepsilon m_\pi^2/M_{QCD}^2) \sim 1\%$. As for the last component of the phenomenological potential, $\mathcal{V}_2^{(2+3)}$ originates entirely from the isospin-violating corrections to the pion and nucleon masses, and it is also relatively small. Note that to this order this component has nothing to do with the coupling \bar{g}_2 of a phenomenological Lagrangian: because of the isoscalar character of the $\bar{\theta}$ term, Eq. (21), \bar{g}_2 arises in EFT only at higher order.

In one-boson-exchange models the $I = 1, 2$ potentials are assumed to arise from pion, eta, rho, and omega isovector and tensor TV couplings to the nucleon [32, 33, 34]. In the ChPT power counting, short-range contributions to these potentials are suppressed with respect to the long-range pieces, again because of the isoscalar character of the $\bar{\theta}$ term. (Of course, because of the factors ε in the long-range

contributions of this order, short-range terms might not be entirely negligible.) This is consistent with the argument that the dominant meson-exchange contributions are from the pion and the eta [32].

There are, therefore, a few points of contact between the local part of our $\nu \leq 3$ potential and the phenomenological potential $V_{T,\min}(\vec{r})$ (92). However, as we have seen in Sects. 4 and 5, at this order EFT yields also momentum-dependent interactions, which in coordinate space appear as non-local potentials and corrections that account for CM motion of the nucleon pair. They can be found in the relativistic and isospin-breaking corrections to OPE in Eqs. (79), (81), and (82).

At $\nu = 3$, the $\bar{\theta}$ two-nucleon potential contains in the CM frame, $\vec{P} = 0$, four spin-isospin structures that are momentum-dependent,

$$\begin{aligned} V_{T,\text{more}}(\vec{r}, \vec{p}_r) = & \frac{g_A \bar{g}_0}{4m_N^2 F_\pi^2} \vec{\tau}^{(1)} \cdot \vec{\tau}^{(2)} \left[\left(\vec{\sigma}^{(1)} - \vec{\sigma}^{(2)} \right) \cdot \left\{ p_r^i, \left\{ p_r^i, \vec{\nabla}_r U(r) \right\} \right\} \right. \\ & - \frac{2}{3} \left(\vec{\nabla}_r^2 U(r) \right) \left(\vec{\sigma}^{(1)} \times \vec{\sigma}^{(2)} \right) \cdot \vec{p}_r + \left(\vec{\sigma}^{(1)} \times \vec{\sigma}^{(2)} \right)^m \left(\nabla_r^m \nabla_r^l U(r) - \frac{1}{3} \delta^{lm} \vec{\nabla}_r^2 U(r) \right) p_r^l \Big] \\ & + \frac{g_A \bar{g}_0 \delta m_N}{2m_N F_\pi^2} \left(\vec{\tau}^{(1)} \times \vec{\tau}^{(2)} \right)_3 \left(\vec{\sigma}^{(1)} + \vec{\sigma}^{(2)} \right) \cdot \{ \vec{p}_r, U(r) \}, \end{aligned} \quad (102)$$

where $\vec{p}_r = -i\vec{\nabla}_r$ denotes the quantum-mechanical relative momentum operator.

The structure of the momentum-dependent TV potentials was considered previously in Ref. [35], where all possible Hermitian operators were constructed, which violate time-reversal and parity, and contain up to one power of momentum \vec{p}_r . The momentum-dependent TV potential was parameterized with eleven unknown functions $d_i(r)$, $i = 1, 2, \dots, 11$. The first term in Eq. (102) is quadratic in the momentum operator and was not considered in Ref. [35]. The second and third spin-isospin structures correspond, respectively, to the isoscalar functions $d_2(r)$ and $d_6(r)$. For TV from the QCD $\bar{\theta}$ term, these two functions are therefore dominated by pion-exchange, and their coefficients are fixed by Lorentz invariance and do not contain any new TV parameter. Isospin-breaking effects in the strong interaction give rise to the last term in Eq. (102), which is proportional to the nucleon mass difference, and it is the first contribution of the $\bar{\theta}$ term to $d_{10}(r)$. Once again, d_{10} is dominated by OPE diagrams, and the only TV parameter intervening is \bar{g}_0 . We find that, at order $\nu = 3$ in ChPT, the other isospin-conserving (the isoscalar d_1 and d_5) and isospin-breaking (d_3, d_4, d_7, d_8, d_9 and d_{11}) functions do not receive contributions from $\bar{\theta}$.

In order to get a sense of the importance of the momentum-dependent contributions, we consider the effect of the relativistic correction in Eq. (102) that is quadratic in \vec{p}_r . In Fig. 8 we compare it (long-dashed-dotted line) to leading OPE (dashed line), medium-range TPE (dashed-dotted line), and pion mass-splitting corrections (double-dotted-dashed line), all applied to a simple bound-state wave function with the scale present in the 1S_0 channel, $a_s = -23.714$ fm:

$$\psi(r) = \frac{\exp(-r/a_s)}{r}. \quad (103)$$

In this qualitative example the relativistic correction cannot be neglected with respect to the other $\nu = 3$ corrections, and we take Fig. 8 as an indication that also in actual calculations of TV observables it would not be advisable to drop the potential in Eq. (102), when the $\bar{\theta}$ potential is needed to next-to-next-to-leading-order accuracy.

Finally, to the same order we find contributions proportional to the CM momentum of the nucleon pair,

$$\begin{aligned} V_{T,\text{CM}}(\vec{r}, \vec{p}_r, \vec{P}) = & \frac{g_A \bar{g}_0}{8m_N^2 F_\pi^2} \vec{\tau}^{(1)} \cdot \vec{\tau}^{(2)} \left\{ \left(\vec{\sigma}^{(1)} + \vec{\sigma}^{(2)} \right) \cdot \left\{ \vec{p}_r, \left(\vec{\nabla}_r U(r) \right) \cdot \vec{P} \right\} \right. \\ & + \varepsilon^{ijk} \left(\sigma^{(1)i} \sigma^{(2)l} + \sigma^{(1)l} \sigma^{(2)i} \right) \left(\nabla_r^l \nabla_r^k U(r) \right) P^j \\ & + \left(\vec{\sigma}^{(1)} - \vec{\sigma}^{(2)} \right) \cdot \left[2 \left(\vec{\nabla}_r U(r) \right) \vec{P}^2 + \vec{P} \left(\vec{\nabla}_r U(r) \right) \cdot \vec{P} + \frac{1}{m_\pi} (\vec{P} \cdot \vec{\nabla}_r)^2 \left(\vec{\nabla}_r U(r) \right) \right] \Big\} \\ & + \frac{g_A \bar{g}_0 \delta m_N}{2m_N F_\pi^2} \left(\vec{\tau}^{(1)} \times \vec{\tau}^{(2)} \right)_3 \left(\vec{\sigma}^{(1)} - \vec{\sigma}^{(2)} \right) \cdot \left[U(r) \vec{P} - \frac{1}{m_\pi} \left(\vec{\nabla}_r \nabla_r^i U(r) \right) P^i \right], \end{aligned} \quad (104)$$

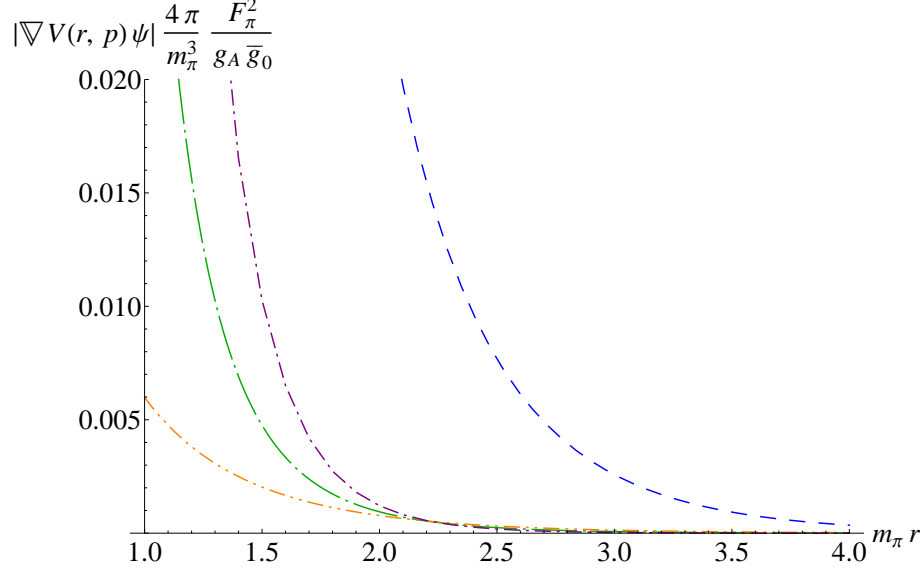


Figure 8: Comparison between a relativistic correction to OPE and local components of the $\bar{\theta}$ two-nucleon potential ∇V_0 applied to an illustrative bound-state wave function ψ , in units of $g_A \bar{g}_0 m_\pi^3 / 4\pi F_\pi^2$, as functions of the distance r , in units of $1/m_\pi$. The (dark green) long-dashed-dotted line represents the term in the potential that is quadratic in momentum. Other curves are as in Fig. 5.

where $\vec{P} = -i\vec{\nabla}_X$. Although the operators in Eq. (104) vanish in the two-nucleon CM frame and are not important for the study of T violation in nucleon-nucleon scattering, they impact observables like TV electromagnetic form factors of the deuteron, where the recoil against the photon changes the CM momentum of the nucleon pair, and they have to be considered in nuclear systems with $A > 2$. An example of the effects of recoil on TC deuteron processes can be found in Compton scattering [86].

At leading order, the dimension-6 sources of TV only contribute to $V_{T,\min}(\vec{r})$, the two-nucleon potential with minimal number of derivatives, in Eq. (92). Combining all these sources,

$$\mathcal{V}_0^{(\nu_{\min})}(r) = -\frac{g_A(3\bar{g}_0 + \bar{g}_2)}{3F_\pi^2} U(r) + \bar{C}_2 \frac{\delta(r)}{8\pi r^2} + \frac{e\bar{d}_1}{24\pi r}, \quad (105)$$

$$\mathcal{U}_0^{(\nu_{\min})}(r) = +\bar{C}_1 \frac{\delta(r)}{8\pi r^2} + \frac{e\bar{d}_0}{8\pi r}, \quad (106)$$

$$\mathcal{V}_1^{(\nu_{\min})}(r) = -\frac{g_A \bar{g}_1}{F_\pi^2} U(r) + \frac{e(\bar{d}_1 - \bar{d}_0)}{8\pi r}, \quad (107)$$

$$\mathcal{U}_1^{(\nu_{\min})}(r) = -\frac{g_A \bar{g}_1}{F_\pi^2} U(r) + \frac{e(\bar{d}_0 + \bar{d}_1)}{8\pi r}, \quad (108)$$

$$\mathcal{V}_2^{(\nu_{\min})}(r) = -\frac{g_A \bar{g}_2}{3F_\pi^2} U(r) + \frac{e\bar{d}_1}{24\pi r}, \quad (109)$$

where

- for qCEDM, $\nu_{\min} = -1$ and only the $\bar{g}_{0,1}$ terms apply;
- for TVCI sources, $\nu_{\min} = -1$ and only the $\bar{g}_{0,1}$ and $\bar{C}_{1,2}$ terms apply; and
- for qEDM, $\nu_{\min} = 2$ and only the $\bar{g}_{0,1,2}$ and $\bar{d}_{0,1}$ terms apply.

In the case of the qCEDM, the potential is thus dominated by OPE, with shorter- or longer-range contributions expected to be small. For the gCEDM and the TV FQ operators, short-range effects are also leading; as for $\bar{\theta}$, these can be parametrized by rho (see Eq. (100)), and eta and/or omega exchange (see Eq. (101)). Only for qEDM all components of $V_{T,\min}(\vec{r})$ appear in leading order thanks to both the most general non-derivative pion-nucleon coupling structure, and to the long-distance potential stemming from the nucleon EDM. The latter cannot be well approximated by heavy-meson exchange.

7 Conclusions

The power-counting scheme of EFTs allows us to organize the contributions to the potential in powers of M_{QCD}^{-1} . The TV PV potential has an ordering that has similarities with the TC PV potential [56]: for all TV sources of dimension up to 6, the leading potential contains one-pion exchange. For T violation from the $\bar{\theta}$ term and from the quark chromo-EDM, the relative importance of two-pion exchange and shorter-range interactions follows the TC PV case closely. However, the situation is different for the quark EDM, the gluon chromo-EDM and TV four-quark operators, where contact interactions or one-photon exchange are relatively more important.

For T violation from the $\bar{\theta}$ term, at leading order, $\mathcal{O}(Q/M_{QCD})$, we find only the well-known OPE from the $I = 0$ pion-nucleon TV coupling [29]. The OPE from the $I = 1$ pion-nucleon TV coupling is suppressed by two orders in the expansion parameter and is of $\mathcal{O}(Q^3/M_{QCD}^3)$. Since the $I = 0$ OPE is suppressed in nuclei, higher orders in the potential could be important. We have thus also examined the corrections in the next two orders, which are up to $\mathcal{O}(Q^2/M_{QCD}^2)$ relative to leading. We have found that the potential is purely two-body, and:

- At the longest, one-pion range, there are more general vertex corrections than usually assumed. We employed the results of Ref. [25] where the TV pion-nucleon vertex was examined to this order. In addition to the qualitatively different $I = 1$ pion-nucleon TV coupling, there are corrections to the local potential stemming from isospin breaking in the pion and nucleon masses, and in the TC pion-nucleon coupling. There are also recoil ($\propto 1/m_N$) and relativistic ($\propto 1/m_N^2$) corrections to leading OPE, which make the potential non-local and dependent on the total momentum of the nucleon pair.
- At this order, we find, additionally, two-pion exchange from the $I = 0$ TV coupling. The non-analytic, medium-range part of the TPE potential is independent of the choice of fields and regulators. Like the leading OPE potential, this part of the TPE potential has as only (so-far) unknown quantity the $I = 0$ TV pion-nucleon coupling. Under reasonable assumptions about the strengths of TV couplings, this potential is stronger, and has a different radial dependence, than phenomenological one-meson-exchange potentials. The main effect of TPE is to modify the potential in the same channels as the leading OPE potential.
- The short-range part of the TPE potential, on the other hand, cannot be separated from contact interactions, the most general form of which we also write at this order. They are two of the terms given in the literature [34]. In the context of a theory without pions, this implies a contribution to only two of five possible S - P transitions. When pions are included explicitly, the short-range terms are expected to be of the same size as TPE, and thus their strengths depend on the renormalization scale. They subsume short-range dynamics that includes the effects of heavier mesons, but whether such effects are sufficient to saturate them is unknown.

The structure of the resulting potential is therefore significantly different than the phenomenological potential used in the literature, due to the specific way in which the $\bar{\theta}$ term breaks chiral symmetry. If consideration of short-range dynamics or $I = 1$ OPE is necessary, one should also include the TPE potential and OPE corrections calculated here.

For the dimension-6 sources, the $I = 1$ pion-nucleon coupling appears already in leading order, $\mathcal{O}(M_{QCD}/Q)$ for qCEDM and chiral-invariant sources (gCEDM and TV FQ) and $\mathcal{O}(Q^2/M_{QCD}^2)$ for qEDM. The structure of the TV potential is thus different from that of $\bar{\theta}$, and depends on the source:

- For qCEDM, it contains only OPE with the well-known $I = 0, 1$ non-derivative pion-nucleon couplings.
- For CI sources, there are, additionally, two contact interactions of the same type as found at next-to-next-to-leading order for $\bar{\theta}$.
- For qEDM, OPE from the three ($I = 0, 1, 2$) non-derivative pion-nucleon couplings is accompanied by one-photon exchange from the nucleon EDM.

Therefore, for all sources we have considered ($\bar{\theta}$, qEDM, qCEDM, gCEDM, and TV FQ), the TV nuclear potential presents more structure (spin, isospin, and/or distance profile) than assumed in the usual phenomenological approach. EFT offers a framework where the calculation of nuclear TV observables can be carried out in a model independent way and characterize the low-energy manifestations of possible TV sources.

Acknowledgments. We thank R. Timmermans for useful discussions. UvK acknowledges the hospitality of the Kavli Institute for Theoretical Physics China and of the Kernfysisch Versneller Instituut at Rijksuniversiteit Groningen during the writing of this paper. This research was supported in part by an APS Forum of International Physics travel grant (CMM, UvK), by FAPERGS-Brazil under contract PROADE 2 02/1266.6 (CMM), by the Brazilian CNPq under contract 474123/2009 (CMM), by the Dutch Stichting voor Fundamenteel Onderzoek der Materie under programme 104 (JdV), and by the US Department of Energy under grants DE-FG02-04ER41338 (EM, UvK) and DE-FG02-06ER41449 (EM).

Appendix: Fourier Transformation to Configuration Space

In general a potential obtained in EFT depends not only on the transferred momentum \vec{q} but also on \vec{K} , and the CM momentum \vec{P} , $V(\vec{q}, \vec{K}, \vec{P})$. The Fourier transform of such a potential is defined as

$$V(\vec{r}, \vec{r}', \vec{X}, \vec{X}') = \int \frac{d^3 K}{(2\pi)^3} \int \frac{d^3 P}{(2\pi)^3} \int \frac{d^3 q}{(2\pi)^3} e^{-i\vec{P} \cdot (\vec{X} - \vec{X}')} e^{-i\vec{K} \cdot (\vec{r} - \vec{r}')} e^{-\frac{i}{2}\vec{q} \cdot (\vec{r} + \vec{r}')} V(\vec{q}, \vec{K}, \vec{P}), \quad (110)$$

where, if \vec{x}_1 and \vec{x}_2 are the positions of the incoming nucleons and \vec{x}'_1 and \vec{x}'_2 the positions of the outgoing nucleons, the relative coordinates are $\vec{r} = \vec{x}_1 - \vec{x}_2$ and $\vec{r}' = \vec{x}'_1 - \vec{x}'_2$, while the CM position of the incoming and outgoing pairs are $2\vec{X} = \vec{x}_1 + \vec{x}_2$ and $2\vec{X}' = \vec{x}'_1 + \vec{x}'_2$. The potential in Eq. (110) has to be used in a two-nucleon Schrödinger equation of the form

$$i \frac{\partial}{\partial t} \psi(\vec{r}', \vec{X}') = - \left(\frac{\vec{\nabla}_{\vec{X}'}^2}{4m_N} + \frac{\vec{\nabla}_{\vec{r}'}^2}{m_N} \right) \psi(\vec{r}', \vec{X}') + \int d^3 \vec{r} \int d^3 \vec{X} V(\vec{r}, \vec{r}', \vec{X}, \vec{X}') \psi(\vec{r}, \vec{X}). \quad (111)$$

For potentials that, like the ones in Sect. 4, are polynomials in \vec{K} and \vec{P} ,

$$V(\vec{q}, \vec{K}, \vec{P}) \propto \vec{K}^m \vec{P}^n f(\vec{q}), \quad (112)$$

$V(\vec{r}, \vec{r}', \vec{X}, \vec{X}')$ assumes the form

$$V(\vec{r}, \vec{r}', \vec{X}, \vec{X}') \propto \left(\vec{\nabla}_{\vec{X}}^n \delta^{(3)}(\vec{X} - \vec{X}') \right) \left(\vec{\nabla}_{\vec{r}}^m \delta^{(3)}(\vec{r} - \vec{r}') \right) f\left(\frac{\vec{r} + \vec{r}'}{2}\right), \quad (113)$$

where

$$f(\vec{r}) = \int \frac{d^3 q}{(2\pi)^3} e^{-i\vec{q} \cdot \vec{r}} f(\vec{q}). \quad (114)$$

Plugging Eq. (113) in Eq. (111), and integrating by parts, the derivatives acting on the delta functions can be turned into derivatives acting on f and on the wave function $\psi(\vec{r}', \vec{X}')$. The integrals in Eq. (111) then become trivial, and the Schrödinger equation assumes the form

$$i \frac{\partial}{\partial t} \psi(\vec{r}', \vec{X}') = - \left(\frac{\vec{\nabla}_{\vec{X}'}^2}{4m_N} + \frac{\vec{\nabla}_{\vec{r}'}^2}{m_N} \right) \psi(\vec{r}', \vec{X}') + V(\vec{r}', \vec{\nabla}_{\vec{r}'}, \vec{\nabla}_{\vec{X}'}) \psi(\vec{r}', \vec{X}'), \quad (115)$$

where the two potentials in Eqs. (111) and (115) are related by integrations by parts. For a potential of the form (112), schematically we would have

$$V(\vec{r}', \vec{\nabla}_{\vec{r}'}, \vec{\nabla}_{\vec{X}'}) \propto (-)^n (-)^m \left\{ \frac{\nabla_{\vec{r}' i_1}}{2}, \dots \left\{ \frac{\nabla_{\vec{r}' i_m}}{2}, f(\vec{r}') \right\} \right\} \nabla_{\vec{X}'}^n, \quad (116)$$

where the indices i_1, \dots, i_m are appropriately contracted.

In order to obtain the potential in configuration space for functions that diverge as the momentum transfer $|\vec{q}|$ goes to infinity, one has to define a regularization scheme. Here, following Ref. [82], we find it convenient to extend the definition of the Fourier transform (114) to a space-time of $d = n + 1$ dimensions:

$$V_n(\vec{r}) = \int \frac{d^n q}{(2\pi)^n} e^{-i\vec{q} \cdot \vec{r}} V(\vec{q}). \quad (117)$$

The amplitude $V(\vec{q})$ is the expression in momentum space of corresponding loop contributions right after the d -dimensional integration over loop momenta is performed, but before setting $d = 4$ or performing the integration over Feynman parameters. Writing

$$d^n q = q^{n-1} dq (1 - \cos^2 \theta)^{\frac{n-3}{2}} d \cos \theta d\Omega_{n-1}, \quad (118)$$

the angular integrations are evaluated with the aid of the formulas

$$\int d\Omega_{n-1} = \frac{2\pi^{\frac{n-1}{2}}}{\Gamma(\frac{n-1}{2})}, \quad (119)$$

and

$$\frac{2\pi^{\frac{n-1}{2}}}{\Gamma(\frac{n-1}{2})} \int_{-1}^1 d \cos \theta (1 - \cos^2 \theta)^{\frac{n-3}{2}} e^{-iqr \cos \theta} = (2\pi)^{\frac{n}{2}} (qr)^{1-\frac{n}{2}} J_{\frac{n}{2}-1}(qr), \quad (120)$$

where $q = |\vec{q}|$, $r = |\vec{r}|$, and $J_n(x)$ denotes a Bessel function of the first kind. For momentum integrals, a useful relation is [87]

$$\int_0^\infty dq q^{\frac{n}{2}} \frac{J_{\frac{n}{2}-1}(qr)}{(q^2 + \beta^2)^{\frac{m-n}{2}}} = \left(\frac{r}{2}\right)^{\frac{m-n}{2}-1} \frac{\beta^{n-\frac{m}{2}}}{\Gamma(\frac{m-n}{2})} K_{\frac{m}{2}-n}(\beta r), \quad (121)$$

where β is a constant and $K_n(x)$ is the modified Bessel function of the second kind.

For example, in the case of the triangle diagrams discussed in Sect. 4,

$$V_\Delta(\vec{q}) = -i \frac{gA\bar{g}_0}{F_\pi^2} \frac{(4\pi\mu^2)^{\frac{3-n}{2}}}{(2\pi F_\pi)^2} \boldsymbol{\tau}^{(1)} \cdot \boldsymbol{\tau}^{(2)} (\vec{\sigma}^{(1)} - \vec{\sigma}^{(2)}) \cdot \vec{q} \Gamma\left(\frac{3-n}{2}\right) \int_0^1 dx [m_\pi^2 + q^2 x(1-x)]^{\frac{n-3}{2}}. \quad (122)$$

For $m = 3$ and $\beta^2 = m_\pi^2/x(1-x)$, the result in Eq. (121) allows one to cancel the divergent factor of $\Gamma((3-n)/2)$ in Eq. (122) and get an expression that is finite for $r \neq 0$. Now we can set $d = 4$ and with the aid of the properties of modified Bessel functions [87] we can write the potential in configuration space as

$$V_\Delta(\vec{r}) = \frac{gA\bar{g}_0}{F_\pi^2} \frac{1}{(2\pi F_\pi)^2} \boldsymbol{\tau}^{(1)} \cdot \boldsymbol{\tau}^{(2)} (\vec{\sigma}^{(1)} - \vec{\sigma}^{(2)}) \cdot \vec{\nabla} \left[\frac{1}{2\pi r^3} \int_0^1 dx (1 + \beta r) e^{-\beta r} \right]. \quad (123)$$

The contributions from box and crossed diagrams can be obtained in a similar fashion, leading to the result in Eq. (85).

Alternatively, we can isolate the short-range, divergent part of the interaction with integration by parts. In Eq. (122), for instance, we then obtain

$$V_{\Delta}(\vec{q}) = -i \frac{g_A \bar{g}_0}{F_{\pi}^2} \frac{(4\pi\mu^2)^{\frac{3-n}{2}}}{(2\pi F_{\pi})^2} \boldsymbol{\tau}^{(1)} \cdot \boldsymbol{\tau}^{(2)} (\vec{\sigma}^{(1)} - \vec{\sigma}^{(2)}) \cdot \vec{q} \left[\Gamma\left(\frac{3-n}{2}\right) m_{\pi}^{n-3} + \Gamma\left(\frac{5-n}{2}\right) \int_0^1 dx \frac{q^2 x(1-2x)}{[m_{\pi}^2 + q^2 x(1-x)]^{\frac{5-n}{2}}} \right]. \quad (124)$$

The first, divergent piece in Eq. (124) is a contribution to a delta-function potential. Applying the d -dimensional Fourier transform to Eq. (124) and taking the $d \rightarrow 4$ limit we find

$$V_{\Delta}(\vec{r}) = \frac{g_A \bar{g}_0}{F_{\pi}^2} \frac{1}{(2\pi F_{\pi})^2} \boldsymbol{\tau}^{(1)} \cdot \boldsymbol{\tau}^{(2)} (\vec{\sigma}^{(1)} - \vec{\sigma}^{(2)}) \cdot \vec{\nabla} \left[\delta^{(3)}(\vec{r}) \left(L + \ln \frac{\mu^2}{m_{\pi}^2} \right) - \frac{1}{4\pi r} \int_0^1 dx \frac{1-2x}{1-x} \beta^2 e^{-\beta r} \right], \quad (125)$$

where L is given in Eq. (57). Proceeding in this way also for box and crossed terms, we find that Fourier transform of the TPE potential can be expressed as

$$V_{TPE}^{(3)}(\vec{r}) = \frac{g_A \bar{g}_0}{F_{\pi}^2} \frac{1}{(2\pi F_{\pi})^2} \boldsymbol{\tau}^{(1)} \cdot \boldsymbol{\tau}^{(2)} (\vec{\sigma}^{(1)} - \vec{\sigma}^{(2)}) \cdot \vec{\nabla} \left\{ -\delta^{(3)}(\vec{r}) \left[(3g_A^2 - 1) \left(L + \ln \frac{\mu^2}{m_{\pi}^2} \right) + 2g_A^2 \right] + \frac{1}{4\pi r} \int_0^1 dx \left[g_A^2 \left(4 - \frac{3}{2x(1-x)} \right) - \frac{1-2x}{1-x} \right] \beta^2 e^{-\beta r} \right\}. \quad (126)$$

The piece proportional to the delta function can then be absorbed in a redefinition of \bar{C}_2 very similar to Eq. (58), the only difference residing in the finite pieces. Integrating by parts, it can be explicitly verified that the non-analytic piece of the expression (126) gives the medium-range potential in the form of Eq. (85).

As a further check of our results, we computed the Fourier transform of the triangle diagrams with a Gaussian regulator $\exp(-q^2/\Lambda^2)$, for different values of the cutoff Λ . The calculation was performed numerically with *Mathematica* [88] and we focused on the region $r > 1/m_{\pi}$. For $\Lambda \simeq m_{\rho}$, the result we get is still quite different from the Fourier transform obtained in dimensional regularization, but as we increase the cutoff to 1–2 GeV, it approximates Eq. (123) better and better.

As pointed out in Ref. [82], in the d -dimensional Fourier-transform procedure the infinities are “regularized” away because the nucleon distance is kept finite. The ultraviolet divergences and the regulator dependence are now hidden in the singular behavior ($\sim 1/r^4$) of the potential for small r , which forces the reintroduction of a regulator in the calculation of matrix elements of $V(r)$. If the chosen regulator were dimensional regularization, then the $d \rightarrow 4$ limit of Eq. (121), which leads to the $1/r^3$ singularity in Eq. (123), must be taken in the sense of generalized functions; the singularity is then encoded by a delta function, proportional to the divergent factor $2/(d-4)$, with a plus distribution remaining [89].

References

- [1] A. Hocker and Z. Ligeti, *Ann. Rev. Nucl. Part. Sci.* **56** (2006) 501.
- [2] H. Nunokawa, S. Parke, and J.W.F. Valle, *Prog. Part. Nucl. Phys.* **60** (2008) 338.
- [3] G. 't Hooft, *Phys. Rev. Lett.* **37** (1976) 8; C.G. Callan, Jr, R.F. Dashen, and D.J. Gross, *Phys. Lett. B* **63** (1976) 334; R. Jackiw and C. Rebbi, *Phys. Rev. Lett.* **37** (1976) 172.

- [4] M. Pospelov and A. Ritz, *Ann. Phys.* **318** (2005) 119.
- [5] C.A. Baker *et al.*, *Phys. Rev. Lett.* **97** (2006) 131801.
- [6] W.C. Griffith *et al.*, *Phys. Rev. Lett.* **102** (2009) 101601.
- [7] V.F. Dmitriev and R.A. Sen'kov, *Phys. Rev. Lett.* **91** (2003) 212303; *Phys. Rev. C* **71** (2005) 035501.
- [8] W. Buchmüller and D. Wyler, *Nucl. Phys. B* **268** (1986) 621 ; A. De Rújula, M.B. Gavela, O. Pène, and F.J. Vegas, *Nucl. Phys. B* **357** (1991) 311 .
- [9] S. Weinberg, *Phys. Rev. Lett.* **63** (1989) 2333 .
- [10] B. Grzadkowski, M. Iskrzynski, M. Misiak, and J. Rosiek, *JHEP* **1010** (2010) 085 .
- [11] M.J. Ramsey-Musolf and S. Su, *Phys. Rept.* **456** (2008) 1 .
- [12] J.S. Nico and W.M. Snow, *Ann. Rev. Nucl. Part. Sci.* **55** (2005) 27.
- [13] T.M. Ito, *J. Phys. Conf. Ser.* **69** (2007) 012037, nucl-ex/0702024.
- [14] K. Bodek *et al.*, arXiv:0806.4837.
- [15] F.J.M. Farley *et al.*, *Phys. Rev. Lett.* **93** (2004) 052001; C.J.G. Onderwater, *J. Phys. Conf. Ser.* **295** (2011) 012008.
- [16] F. Berruto, T. Blum, K. Orginos, and A. Soni, *Phys. Rev. D* **73** (2006) 054509; E. Shintani, S. Aoki, and Y. Kuramashi, *Phys. Rev. D* **78** (2008) 014503; S. Aoki *et al.*, arXiv:0808.1428.
- [17] S. Weinberg, *Physica* **96A** (1979) 327.
- [18] J. Gasser and H. Leutwyler, *Ann. Phys.* **158** (1984) 142; *Nucl. Phys. B* **250** (1985) 465.
- [19] V. Bernard, N. Kaiser, and U.-G Meißner, *Int. J. Mod. Phys. E* **4** (1995) 193.
- [20] R.J. Crewther, P. Di Vecchia, G. Veneziano, and E. Witten, *Phys. Lett. B* **88** (1979) 123; **91** (1980) 487 (E).
- [21] H.-Y. Cheng, *Phys. Rev. D* **44** (1991) 166; A. Pich and E. de Rafael, *Nucl. Phys. B* **367** (1991) 313; P. Cho, *Phys. Rev. D* **48** (1993) 3304; B. Borasoy, *Phys. Rev. D* **61** (2000) 114017; S. Narison, *Phys. Lett. B* **666** (2008) 455.
- [22] S. Thomas, *Phys. Rev. D* **51** (1995) 3955.
- [23] W.H. Hockings and U. van Kolck, *Phys. Lett. B* **605** (2005) 273; K. Ottnad, B. Kubis, U.-G. Meißner, and F.-K. Guo, *Phys. Lett. B* **687** (2010) 42; E. Mereghetti, J. de Vries, W.H. Hockings, C.M. Maekawa, and U. van Kolck, *Phys. Lett. B* **696** (2011) 97.
- [24] J. de Vries, E. Mereghetti, R.G.E. Timmermans, and U. van Kolck, *Phys. Lett. B* **695** (2011) 268
- [25] E. Mereghetti, W.H. Hockings, and U. van Kolck, *Ann. Phys.* **325** (2010) 2363.
- [26] J. de Vries, E. Mereghetti, R.G.E. Timmermans, and U. van Kolck, in preparation.
- [27] O. Lebedev, K.A. Olive, M. Pospelov, and A. Ritz, *Phys. Rev. D* **70** (2004) 016003.
- [28] J. de Vries, E. Mereghetti, R.G.E. Timmermans, and U. van Kolck, arXiv:1102.4068
- [29] W.C. Haxton and E.M. Henley, *Phys. Rev. Lett.* **51** (1983) 1937.
- [30] P. Herczeg, in *Tests of Time-Reversal Invariance in Neutron Physics*, N.R. Robertson, C.R. Gould, and J.D. Bowman (editors), World Scientific, Singapore (1987).

- [31] G. Barton, *Nuovo Cim.* **19** (1961) 512.
- [32] V.P. Gudkov, X.-G. He, and B.H.J. McKellar, *Phys. Rev. C* **47** (1993) 2365.
- [33] I.S. Towner and A.C. Hayes, *Phys. Rev. C* **49** (1994) 2391.
- [34] C.-P. Liu and R.G.E. Timmermans, *Phys. Rev. C* **70** (2004) 055501.
- [35] P. Herczeg, *Nucl. Phys.* **75** (1966) 665.
- [36] B. Desplanques, J.F. Donoghue, and B.R. Holstein, *Ann. Phys.* **124** (1980) 449.
- [37] Y. Avishai, *Phys. Rev. D* **32** (1985) 314.
- [38] Y. Avishai and M. Fabre de la Ripelle, *Phys. Rev. Lett.* **56** (1986) 2121.
- [39] I.B. Khriplovich and R.V. Korkin, *Nucl. Phys. A* **665** (2000) 365; R.V. Korkin, nucl-th/0504078.
- [40] I. Stetcu, C.-P. Liu, J.L. Friar, A.C. Hayes, and P. Navrátil, *Phys. Lett. B* **665** (2008) 168.
- [41] A. Griffiths and P. Vogel, *Phys. Rev. C* **43** (1991) 2844.
- [42] V.V. Flambaum, I.B. Khriplovich, and O.P. Sushkov, *Sov. Phys. JETP* **60** (1984) 873; *Phys. Lett. B* **162** (1985) 213; *Nucl. Phys. A* **449** (1986) 750.
- [43] J. Dobaczewski and J. Engel, *Phys. Rev. Lett.* **94** (2005) 232502; J.H. de Jesus and J. Engel, *Phys. Rev. C* **72** (2005) 045503.
- [44] P. Herczeg, in *Symmetries and Fundamental Interactions in Nuclei*, W.C. Haxton and E.M. Henley (editors), World Scientific, Singapore (1995).
- [45] V.P. Gudkov, *Phys. Rep.* **212** (1992) 77.
- [46] C.-P. Liu and R.G.E. Timmermans, *Phys. Lett. B* **634** (2006) 488.
- [47] Y.-H. Song, R. Lazauskas, and V. Gudkov, arXiv:1104.3051 [nucl-th].
- [48] U. van Kolck, *Prog. Part. Nucl. Phys.* **43** (1999) 337; P.F. Bedaque and U. van Kolck, *Ann. Rev. Nucl. Part. Sci.* **52** (2002) 339; E. Epelbaum, H.-W. Hammer, and U.-G. Meißner, *Rev. Mod. Phys.* **81** (2009) 1773.
- [49] C. Ordóñez and U. van Kolck, *Phys. Lett. B* **291** (1992) 459; C. Ordóñez, L. Ray, and U. van Kolck, *Phys. Rev. Lett.* **72** (1994) 1982; *Phys. Rev. C* **53** (1996) 2086; N. Kaiser, R. Brockmann, and W. Weise, *Nucl. Phys. A* **625** (1997) 758; N. Kaiser, S. Gerstendorfer, and W. Weise, *Nucl. Phys. A* **637** (1998) 395; J.L. Friar, *Phys. Rev. C* **60** (1999) 034002.
- [50] U. van Kolck, *Phys. Rev. C* **49** (1994) 2932; J.L. Friar, D. Hüber, and U. van Kolck, *Phys. Rev. C* **59** (1999) 53; E. Epelbaum, A. Nogga, W. Glöckle, H. Kamada, U.-G. Meißner, and H. Witała, *Phys. Rev. C* **66** (2002) 064001.
- [51] U. van Kolck, J.L. Friar, and T. Goldman, *Phys. Lett. B* **371** (1996) 169.
- [52] U. van Kolck, M.C.M. Rentmeester, J.L. Friar, T. Goldman, and J.J. de Swart, *Phys. Rev. Lett.* **80** (1998) 4386; N. Kaiser, *Phys. Rev. C* **73** (2006) 044001.
- [53] J.L. Friar and U. van Kolck, *Phys. Rev. C* **60** (1999) 034006; J.A. Niskanen, *Phys. Rev. C* **65** (2002) 037001; J.L. Friar, U. van Kolck, G.L. Payne, and S.A. Coon, *Phys. Rev. C* **68** (2003) 024003.
- [54] J.L. Friar, U. van Kolck, M.C.M. Rentmeester, and R.G.E. Timmermans, *Phys. Rev. C* **70** (2004) 044001.

- [55] E. Epelbaum, U.-G. Meißner, and J.E. Palomar, *Phys. Rev. C* **71** (2005) 024001; J.L. Friar, G.L. Payne, and U. van Kolck, *Phys. Rev. C* **71** (2005) 024003.
- [56] S.-L. Zhu, C.M. Maekawa, B.R. Holstein, M.J. Ramsey-Musolf, and U. van Kolck, *Nucl. Phys. A* **748** (2005) 435.
- [57] N. Kaiser, *Phys. Rev. C* **76** (2007) 047001; Y.-R. Liu and S.-L. Zhu, *Chin. Phys.* **32** (2008) 700; L. Girlanda, *Phys. Rev. C* **77** (2008) 067001.
- [58] H.W. Griedhammer and M.R. Schindler, *Eur. Phys. J. A* **46** (2010) 73.
- [59] D.B. Kaplan and M.J. Savage, *Nucl. Phys. A* **556** (1993) 653; **570** (1994) 833 (E); **580** (1994) 679 (E); C.M. Maekawa and U. van Kolck, *Phys. Lett. B* **478** (2000) 73; C.M. Maekawa, J.S. da Veiga, and U. van Kolck, *Phys. Lett. B* **488** (2000) 167; P.F. Bedaque and M.J. Savage, *Phys. Rev. C* **62**, 018501 (2000); S.-L. Zhu, C.M. Maekawa, B.R. Holstein, and M.J. Ramsey-Musolf, *Phys. Rev. Lett.* **87** (2001) 201802; S.-L. Zhu, C.M. Maekawa, G. Sacco, B.R. Holstein, and M.J. Ramsey-Musolf, *Phys. Rev. D* **65** (2002) 033001.
- [60] B.R. Holstein, *Fizika B* **14** (2005) 165; D.R. Phillips, M.R. Schindler, and R.P. Springer, *Nucl. Phys. A* **822** (2009) 1; J.W. Shin, S. Ando, and C.H. Hyun, *Phys. Rev. C* **81** (2010) 055501; M.R. Schindler and R.P. Springer, *Nucl. Phys. A* **846** (2010) 51.
- [61] C.-P. Liu, *Phys. Rev. C* **75** (2007) 065501; C.H. Hyun, S. Ando, and B. Desplanques, *Eur. Phys. J. A* **32** (2007) 513; *Phys. Lett. B* **651** (2007) 257; J.A. Niskanen, T.M. Partanen, and M.J. Iqbal, *Eur. Phys. J. A* **36** (2008) 295; B. Desplanques, C.H. Hyun, S. Ando, and C.-P. Liu, *Phys. Rev. C* **77** (2008) 064002; R. Schiavilla, M. Viviani, L. Girlanda, A. Kievsky, and L.E. Marcucci, *Phys. Rev. C* **78** (2008) 014002; M. Viviani, R. Schiavilla, L. Girlanda, A. Kievsky, and L.E. Marcucci, *Phys. Rev. C* **82** (2010) 044001.
- [62] S. Weinberg, *The Quantum Theory of Fields*, Vol. 2 (Cambridge University Press, Cambridge, 1996).
- [63] E. Jenkins and A.V. Manohar, *Phys. Lett. B* **255** (1991) 558.
- [64] U. van Kolck, Ph.D. dissertation, University of Texas (1993); *Few-Body Syst. Suppl.* **9** (1995) 444.
- [65] A. Manohar and H. Georgi, *Nucl. Phys. B* **234** (1984) 189.
- [66] S. Weinberg, *Phys. Lett. B* **251** (1990) 288; *Nucl. Phys. B* **363** (1991) 3.
- [67] S.R. Beane, P.F. Bedaque, L. Childress, A. Kryjevski, J. McGuire, and U. van Kolck, *Phys. Rev. A* **64** (2001) 042103.
- [68] S.R. Beane, P.F. Bedaque, M.J. Savage, and U. van Kolck, *Nucl. Phys. A* **700** (2002) 377; A. Nogga, R.G.E. Timmermans, and U. van Kolck, *Phys. Rev. C* **72** (2005) 054006; M.C. Birse, *Phys. Rev. C* **74** (2006) 014003; *Phys. Rev. C* **76** (2007) 034002; M. Pavón Valderrama and E. Ruiz Arriola, *Phys. Rev. C* **74** (2006) 064004.
- [69] B. Long and U. van Kolck, *Ann. Phys.* **323** (2008) 1304.
- [70] M. Pavón Valderrama, *Phys. Rev. C* **83** (2011) 024003.
- [71] V. Bernard, N. Kaiser, J. Kambor, and U.-G. Meißner, *Nucl. Phys. B* **388** (1992) 315; N. Fettes, U.-G. Meißner, and S. Steininger, *Nucl. Phys. A* **640** (1998) 199.
- [72] K. Nakamura [Particle Data Group], *J. Phys. G* **37** (2010) 075021.
- [73] S.R. Beane, K. Orginos, and M.J. Savage, *Nucl. Phys. B* **768** (2007) 38.

- [74] U. van Kolck, J.A. Niskanen, and G.A. Miller, *Phys. Lett. B* **493** (2000) 65; D.R. Bolton and G.A. Miller, *Phys. Rev. C* **81** (2010) 014001; A. Filin *et al.*, *Phys. Lett. B* **681** (2009) 423.
- [75] J. Gasser and H. Leutwyler, *Phys. Rep.* **87** (1982) 77.
- [76] V. Baluni, *Phys. Rev. D* **19** (1979) 2227.
- [77] S.A. Coon, B.H.J. McKellar, and V.C.J. Stoks, *Phys. Lett. B* **385** (1996) 25.
- [78] U. van Kolck, hep-ph/9711222; *Nucl. Phys. A* **645** (1999) 273.
- [79] D.B. Kaplan, M.J. Savage, and M.B. Wise, *Nucl. Phys. B* **534** (1998) 329.
- [80] T.S. Park, D.P. Min, and M. Rho, *Phys. Rept.* **233** (1993) 341.
- [81] V.G.J. Stoks, R. Timmermans, and J.J. de Swart, *Phys. Rev. C* **47** (1993) 512; M.C.M. Rentmeester, R.G.E. Timmermans, J.L. Friar, and J.J. de Swart, *Phys. Rev. Lett.* **82** (1999) 4992.
- [82] J.L. Friar, *Mod. Phys. Lett. A* **11** (1996) 3043.
- [83] V.G.J. Stoks, R.A.M. Klomp, C.P.F. Terheggen, and J.J. de Swart, *Phys. Rev. C* **49** (1994) 2950; R. Machleidt, *Phys. Rev. C* **63** (2001) 024001.
- [84] L. Tiator, C. Bennhold, and S.S. Kamalov, *Nucl. Phys.* **A580** (1994) 455.
- [85] M. Hoferichter, B. Kubis and U.-G. Meißner, *Nucl. Phys. A* **833** (2010) 18.
- [86] S.R. Beane, M. Malheiro, J.A. McGovern, D.R. Phillips, and U. van Kolck, *Nucl. Phys. A* **747** (2005) 311.
- [87] M. Abramowitz and I. Stegun, *Handbook of Mathematical Functions* (Dover, New York, 1965); I.S. Gradshteyn and I.M. Ryzhik, *Table of Integrals, Series and Products*, Fifth Edition, Ed. A. Jeffrey (Academic Press, Boston, 1994).
- [88] Wolfram Research, Inc., *Mathematica*, Version 7.0 (Champaign, 2008).
- [89] I.M. Gelfand and G.E. Shilov, *Generalized Functions*, Vol. 1 (Academic Press, New York, 1964).